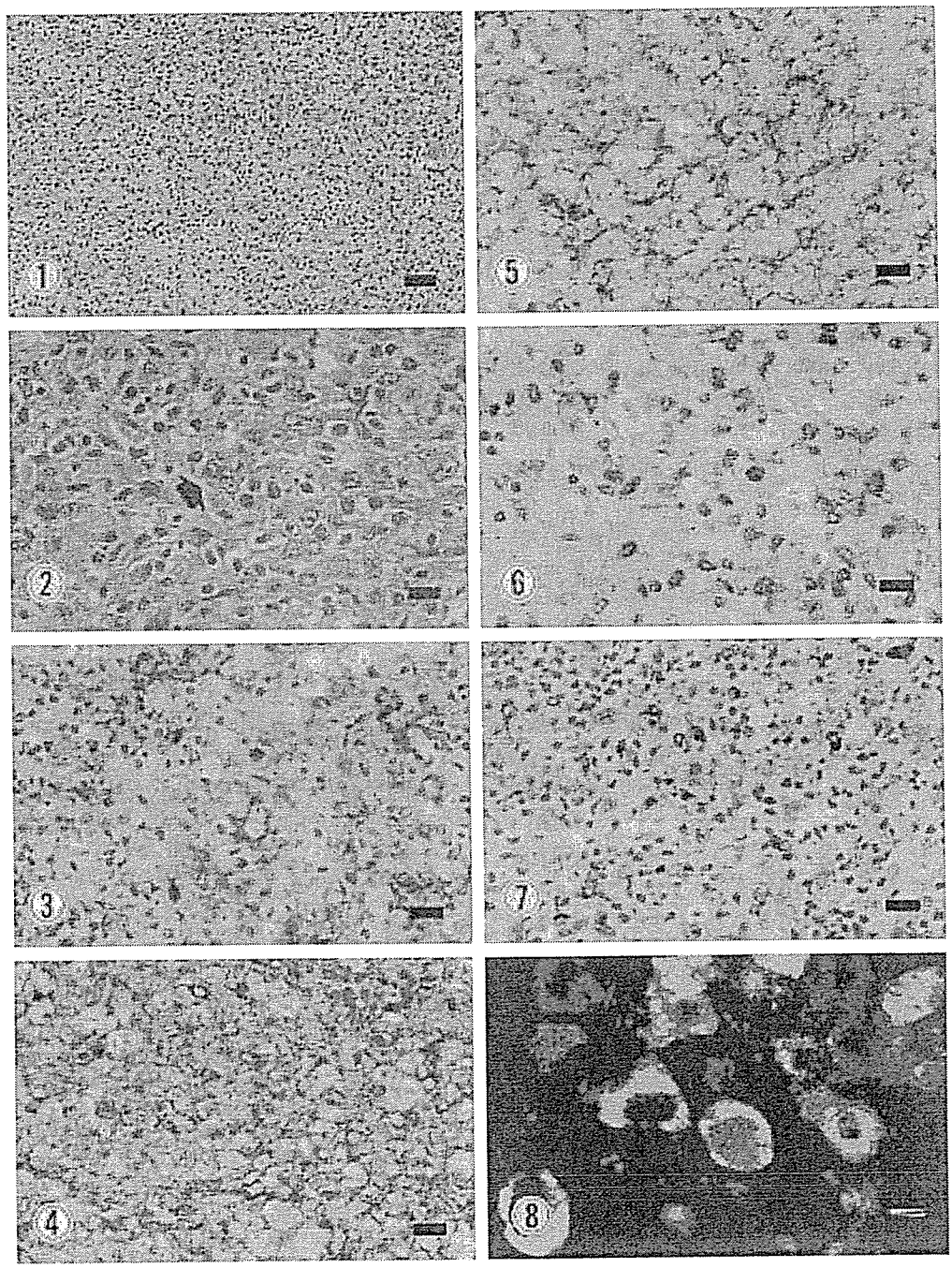

Fig. 1. Histology of the buccal mass in the cynomolgus monkey. Neoplastic large cells are intermingled with reactive small cells. Bar=40 μm. HE.

Fig. 2. Higher magnification of Fig. 1. In addition to neoplastic large cells and reactive small cells, a multinucleated giant cell (arrow) is seen. Bar=10 μm. HE.

Fig. 3. Immunostain for CD20. The majority of large cells show positive reaction. Bar=10 μm. Methylgreen counterstain.

Fig. 4. Immunostain for IgG. Most large cells show positive reaction. Bar=10 μm. Methylgreen counterstain.

Fig. 5. Immunostain for HLA-DR. The majority of large cells and small cells show positive reaction. Bar=10 μm. Methylgreen counterstain.

Fig. 6. Immunostain for CD3. The majority of small cells show positive reaction. Bar=10 μm. Methylgreen counterstain.

Fig. 7. Immunostain for lysozyme. Some small cells show positive reaction. Bar=10 μm. Methylgreen counterstain.

Fig. 8. Double-labeled immunoflorecsence method. Neoplastic large cells are positive for IgA (green) or IgG (red), or both (yellow). Bar=5 μm.

cells in the buccal mass and mandibular lymph node.

Lymphomas showing a wide range of diverse morphology are well known in various mammalian species [18]. Furthermore, they have been immunohistochemically subclassified using lymphocytic subset markers [10]. In humans, TCRBCL is characterized by an admixture of large-sized neoplastic B-cells and small-sized reactive T-cells and the latter comprises more than 50% of the whole cellular population [19]. This type of lymphoma has been reported not only in humans [3, 19–21], but also in other mammalian species including dog [2], cat [6, 23], pig [26], and horse [17]. Histological features of TCRBCL in these animals are considered to be very similar to those of human TCRBCL.

In the present case, neoplastic large lymphoid cells, giant cells and reactive small mononuclear cells were observed. Neoplastic large lymphoid cells and giant cells showed B-cell markers, such as CD20, CD79α, Igs and HLA-DR, and the majority of the small mononuclear cells were CD3-positive and partly HLA-DR-positive reactive T-cells. These characteristics are consistent with those of TCRBCL in humans [3, 19–21]. However, in the present case some of the small-sized cells were positive for B-cell markers (CD20, CD79α) or histiocytic markers (HAM56, MAC387). Such a variety of reactive cells has not been confirmed in TCRBCLs reported in humans and other mammalian species [2, 3, 6, 17, 20, 21, 23, 26]. The difference between human and cynomolgus monkey may be due to different cytokine profiles produced by neoplastic B-cells.

Most B-cell lymphomas produce only a subclass of Ig, since all tumor cells usually originate from a single cell. The monoclonality of large B-cells in human TCRBCL has been reported in most cases, whereas polyclonality in TCRBCL has been demonstrated only in a pig [26]. The present study demonstrated polyclonal Ig production in B-cell lymphoma of a non-human primate using immunostains and the dl-IF method. These findings suggest that the neoplastic B-cells in this tumor may have produced polyclonal Ig. However, whether the neoplastic B-cells expressed Ig-κ and -λ remained to be confirmed. A relationship between EBV and oncogenesis was not demonstrated in the present case.

Acknowledgments

The authors thank Rieko Kobayashi for her technical help.

References

1. Anderson, W.I., Inhelder, J.L., and King, N.W, Jr. 1994. *J. Med. Primatol.* 23: 56–57.
2. Aquino, S.M., Hamor, R.E., Valli, V.E., Kitchell, B.E., Tunev, S.S., Bailey, K.L., and Ehrhart, E.J. 2000. *Vet. Pathol.* 37: 465–469.
3. Baddoura, F.K., Chan, W.C., Masih, A.S., Mitchell, D., Sun, N.C.J., and Weisenburger, D.D. 1995. *Am. J. Cli. Pathol.* 103: 65–75.
4. Binhazim, A.A., Lee, D.R., Bernacky, B.J., and Rizvi, T.A. 1997. *J. Med. Primatol.* 26: 260–266.
5. Chang, K.L., Chen, Y-Y., Shibata, D., and Weiss, L.M. 1992. *Diagn. Mol. Pathol.* 1: 246–255.
6. Day, M.J., Kyaw-Tanner, M., Silkstone, M.A., Lucke, V.M., and Robinson, W.F. 1999. *J. Comp. Path.* 120: 155–167.
7. De Paoli, A. and Garner, F.M. 1968. *Cancer Res.* 28: 2559–2561.
8. Goldberg, R.J., Scolnick, E.M., Parks, W.P., Yakovleva, L.A., and Lapin, B.A. 1974. *Int. J. Cancer* 14: 722–730.
9. Fujimoto, K and Honjo, S. 1991. *J. Med. Primatol.* 20: 42–45.
10. Harris, N.L., Jaffe, E.S., Stein, H., Banks, P.M., Chan, J.K.C., Cleary, M.L., Delsol, G., De Wolf-Peeters, C., Falini, B., Gatter, K.C., Grogan, T.M., Isaacson, P.G., Knowles, D.M., Mason, D.Y., Muller-Hermelink, H-K., Pileri, S.A., Piris, M.A., Ralfkiaer, E., and Warnke, R.A. 1994. *Blood* 84: 1361–1392.
11. Hayashi, K., Chen, H-L., Yanai, H., Koirala, T.R., Ohara, N., Teramoto, N., Oka, T., Yoshino, T., Takahashi,. K., Miyamoto, K., Fujimoto, K., Yoshikawa, Y., and Akagi, T. 1999. *Lab. Invest.* 79: 823–835.
12. Hofmann, P., Kahnt, K., Mätz-Rensing, K., Brack, M., and Kaup, F-J. 2001. *J. Med. Primatol.* 30: 322–327.
13. Hubbard, G.B., Moné, J.P., Allan, J. S., Davis, K.J., III., Michelle Leland, M., Banks, P.M., and Smir, B. 1993. *Lab. Anim. Sci.* 43: 301–309.
14. Jaax, N.K., Petrali, J.P., and Jaax, J.P. 1988. *Lab. Anim. Sci.* 38: 198–200.
15. Johnsen, D.O., Wooding, W.L., Tanticharoenyos, P., and Bourgeois, C.H,Jr. 1971. *J. Am. Vet. Med. Assoc.* 159: 563–566.
16. Jones, M.D., Lau, D.T., and Warthen, J. 1972. *J. Natl. Cancer Inst.* 49: 599–601.
17. Kelley, L.C. and Mahaffey, E.A. 1998. *Vet. Pathol.* 35: 241–252.
18. Moulton, J.K. Tumor in domestic animals. Third edition, revised and expanded; Tumor of the lymphoid and hematopoietic. pp. 231–307.
19. Ng, C.S., Chan, J.K.C., Hui, P.K., and Lau, W.H. 1989. *Hum. Pathol.* 20: 1145–1154.

20. Ramsay, A.D., Smith, W.J., and Isaacson, P.G. 1998. *Am. J. Surg. Pathol.* 12: 433–443.
21. Rodriquoz, J., Pugh, W.C., and Cabanillas, F. 1993. *Blood* 82: 1586–1589.
22. Sakakibara, I., Sugimoto, Y., Sasagawa, A., Honjo, S., Tsujimoto, H., Nakamura, H., and Hayashi, M. 1986. *J. Med. Primatol.* 15: 311–318.
23. Steele, K.E., Saunders, G.K., and Coleman, G.D. 1997. *Vet. Pathol.* 34: 47–49.
24. Stowell, R.E., Smith, E.K., España, C., and Nelson., V.G. 1971. *Lab. Invest.* 25: 476–479.
25. Take, H., Kubota, K., Fukuda, T., Shinonome, S., Ishikawa, O., and Shirakura, T. 1996. *Am. J. Hematol.* 52: 221–223.
26. Tanimoto, T. and Ohtsuki, Y. 1998. *Vet. Pathol.* 35: 147–149.
27. Wakatsuki, S., Yumoto, N., Takagi, T., Kurosu, K., Sakai, C., Tamayama, C., Komatsu, T., Matsuzaki, O., and Mikata, A. 1995. *Pathol. Int.* 45: 457–462.

ACADEMIC PRESS

Available online at www.sciencedirect.com

SCIENCE DIRECT®

Biochemical and Biophysical Research Communications 304 (2003) 176–183

BBRC

www.elsevier.com/locate/ybbrc

Alterations of structure and hydrolase activity of parkinsonism-associated human ubiquitin carboxyl-terminal hydrolase L1 variants

Kaori Nishikawa,[a,b] Hang Li,[a] Ryoichi Kawamura,[c] Hitoshi Osaka,[a,d] Yu-Lai Wang,[a] Yoko Hara,[a,b] Takatsugu Hirokawa,[e] Yoshimasa Manago,[f] Taiju Amano,[f] Mami Noda,[f] Shunsuke Aoki,[a] and Keiji Wada[a,*]

[a] *Department of Degenerative Neurological Diseases, National Institute of Neuroscience, National Center of Neurology and Psychiatry, 4-1-1 Ogawahigashi, Kodaira, Tokyo 187-8502, Japan*

[b] *Japan Science and Technology Corporation (JST), Kawaguchi, Saitama 332-0012, Japan*

[c] *Blood Products Research Department, The Chemo-Sero-Therapeutic Research Institute, Kumamoto 869-1298, Japan*

[d] *Precursory Research for Embryonic Science and Technology (PRESTO), JST, Kawaguchi, Saitama 332-0012, Japan*

[e] *Computational Biology Research Center (CBRC), National Institute of Advanced Industrial Science and Technology (AIST), Tokyo 135-0064, Japan*

[f] *Laboratory of Pathophysiology, Graduate School of Pharmaceutical Sciences, Kyushu University, Fukuoka 812-8582, Japan*

Received 14 March 2003

Abstract

Ubiquitin carboxyl-terminal hydrolase L1 (UCH-L1) is a neuron-specific ubiquitin recycling enzyme. A mutation at residue 93 and polymorphism at residue 18 within human UCH-L1 are linked to familial Parkinson's disease and a decreased Parkinson's disease risk, respectively. Thus, we constructed recombinant human UCH-L1 variants and examined their structure (using circular dichroism) and hydrolase activities. We confirmed that an I93M substitution results in a decrease in k_{cat} (45.6%) coincident with an alteration in α-helical content. These changes may contribute to the pathogenesis of Parkinson's disease. In contrast, an S18Y substitution results in an increase in k_{cat} (112.6%) without altering the circular dichroistic spectrum. These data suggest that UCH-L1 hydrolase activity may be inversely correlated with Parkinson's disease risk and that the hydrolase activity is protective against the disease. Furthermore, we found that oxidation of UCH-L1 by 4-hydroxynonenal, a candidate for endogenous mediator of oxidative stress-induced neuronal cell death, results in a loss of hydrolase activity. Taken together, these results suggest that further studies of altered UCH-L1 hydrolase function may provide new insights into a possible common pathogenic mechanism between familial and sporadic Parkinson's disease.

Keywords: Ubiquitin; Proteasome; UCH-L1; Parkinsonism; Oxidative stress; 4-Hydroxynonenal

The ubiquitin–proteasome system is an evolutionarily conserved and energy-dependent proteolytic pathway. In addition to the elimination of misfolded and damaged toxic proteins produced in response to various cellular stresses, this pathway is responsible for turnover of various classes of short-lived proteins that control cell-cycle progression, specific gene transcription, membrane protein traffic, and intracellular signaling [1–4]. Ubiquitination of proteins is mediated by specific enzymes (E1, E2, and E3), and polyubiquitinated proteins are translocated to the proteasome and subsequently proteolytically degraded [3]. Conversely, deubiquitination is thought to be essential for the negative regulation of proteolysis and for recycling of ubiquitin from polyubiquitin chains [5].

Deubiquitinating enzymes consist of at least two families: the UBP (ubiquitin-specific processing protease) family [6–9] and the UCH family [7,8]. UBPs are thought to disassemble polyubiquitin chains whereas

* Corresponding author. Fax: +81-42-346-1745.
E-mail address: wada@ncnp.go.jp (K. Wada).

0006-291X/03/$ - see front matter © 2003 Elsevier Science (USA). All rights reserved.
doi:10.1016/S0006-291X(03)00555-2

UCHs hydrolyze only small C-terminal ubiquitin adducts [8–10]. This restricted substrate specificity led to the proposal that UCHs function in ubiquitin recycling rather than in deubiquitination [11,12]. To date, four isoforms of UCH, L1–L4, have been identified in mammals [13–15].

Of the four UCH isoforms, UCH-L1 is neuron-specific [16,17]. Mutant mice with an intragenic deletion of the *UCH-L1* gene display neuron subtype-specific phenotypes and severe neurodegenerative disorders including gracile axonal dystrophy [18]. Previous studies of *UCH-L1*-associated human neurodegenerative diseases revealed single amino acid changes within UCH-L1 in some patients with Parkinson's disease (PD). An I93M missense mutation was identified in a German family affected by PD, and the partial loss of UCH-L1 hydrolase activity in this mutant may contribute to the disease [19]. Furthermore, an S18Y polymorphism encoded in exon 3 of human *UCH-L1* may be associated with decreased risk of PD in Caucasian, German, and Japanese populations [20–24] although no such association has been identified in other populations [25–28]. Recently, a novel enzymatic activity of UCH-L1 was discovered that affects the degradation of α-synuclein, a core component of Lewy bodies. The study demonstrated that the UCH-L1 dimer exhibits an ATP-independent ubiquitin ligase activity that inhibits the degradation of ubiquitinated α-synuclein (ubiquitinated at Lys 63) [29]. Furthermore, S18Y UCH-L1 ligase activity is lower than that of the wild-type enzyme, suggesting a possible link between the ligase activity and lowered risk of PD [29].

Although the I93M mutation and S18Y polymorphism of UCH-L1 could affect a single factor in the etiology of PD, common functional changes between the I93M and S18Y mutants of UCH-L1 have not been reported. In the present study, we reveal that UCH-L1 hydrolase activity is altered in both the I93M and S18Y UCH-L1 variants, suggesting that the pathogenesis of PD in both cases may have a common origin. We further demonstrate that UCH-L1 hydrolase activity is decreased by treatment with 4-hydroxynonenal (HNE), a candidate for endogenous mediator of oxidative stress-induced neuronal cell death, which is associated with sporadic PD. Thus, the hydrolase activity may also be involved in the pathogenesis of sporadic PD. Moreover, we also reveal that I93M UCH-L1 exhibits altered α-helical content relative to wild-type UCH-L1.

Materials and methods

Cloning of human UCH-L1. Human *UCH-L1* cDNA (GenBank Accession No. BC006305) was amplified by PCR using a human brain cDNA pool (Stratagene, La Jolla, CA) as template with the following primer sets: forward primer, 5′-GGGGCTCGAGCCGCGAAGAT GCAGCTCAAGCCGATGGAGATCAACCCCGAGATGCTGA-3′ (5′-GGGG-*Xho*I-CCGCGAAG-Met[1]-Gln-Leu-Lys-Pro-Met-Glu-Ile-Asn-Pro-Glu-Met-Leu[13]-3′), and reverse primer, 5′-GGGGGCGG CCGCTTAGGCTGCCTTGCAGAGAGCCA-3′ (3′-Ala[226]-Leu-Cys-Lys-Ala-Ala[233]-stop-*Not*I-GGGG-5′). Following an initial 3 min denaturation at 95 °C, the sample was amplified by 30 cycles of denaturation at 95 °C for 10 s, annealing at 53 °C for 20 s, and extension at 72 °C for 30 s. The amplified fragment was digested with *Xho*I and *Not*I and subcloned into the *Xho*I and *Not*I sites of pCI-neo (Promega, Madison, WI). Accuracy of the inserted nucleotide sequence was confirmed by sequence analysis.

Construction of bacterial expression plasmids for human UCH-L1 variants. Mutant cDNAs encoding human UCH-L1 containing either the I93M, S18Y, or C90S substitution were obtained using the QuikChange site-directed mutagenesis kit (Stratagene) with the following mutagenesis oligonucleotides: 5′-GAATTCCTGTGGCACAATG GGACTTATTCACGCAG-3′ and 5′-CTGCGTGAATAAGTCCC ATTGTGCCACAGGAATTC-3′ for I93M; 5′-GAACAAAGTGC TGTCCCGGCTGGGGGTCGC-3′ and 5′-GCGACCCCCAGCCGG GACAGCACTTTGTTC-3′ for S18Y; and 5′-CCATTGGGAAT TCCTCTGGCACAATCGGAC-3′ and 5′-GTCCGATTGTGCCA CAGGAATTCCCAATGG-3′ for C90S. Each single-nucleotide mutation in the resulting plasmids was confirmed by sequencing. Bacterial expression plasmids containing either 6HN-tagged human UCH-L1, I93M, S18Y, or C90S were constructed using a tetracycline-inducible expression system. *Xho*I–*Not*I cDNA fragments of the pCI-neo human UCH-L1 and mutant were digested, and then the DNA fragments were ligated between the *Sal*I and *Not*I sites in pPROtetE233 (Clontech, Palo Alto, CA) to generate pPROtetE233 6HN-tagged human UCH-L1, I93M, S18Y, and C90S vectors. The veracity of these expression plasmids was confirmed by sequencing.

Preparation of recombinant proteins. The pPROtetE233 6HN-tagged human UCH-L1, I93M, S18Y, and C90S vectors were transformed into *Escherichia coli* DH5αPRO. Purification of the recombinant proteins was performed using Co^{2+}–Sepharose (TALON purification kit, Clontech) according to the manufacturer's instructions.

Protein concentrations were determined using the BCA protein assay reagent (Pierce). Purified proteins were resolved by SDS–PAGE (sodium dodecyl sulfate–polyacrylamide gel electrophoresis) under reducing conditions and visualized by Coomassie brilliant blue R-250 to confirm purity.

In vitro assay for human UCH-L1 activity. The hydrolase assay was performed as described in [30] with slight modifications. The assay for human UCH-L1 was carried out using a 96-well black assay plate at room temperature. Purified enzymes and the fluorogenic substrate ubiquitin-7-amino-4-methylcoumarin (Ub-AMC) (Boston Biochem, Cambridge, MA) were used to determine steady state kinetic parameters. The final enzyme concentration was 4.3 nM for UCH-L1, I93M, and S18Y mutants, and 5 μM for C90S. Before adding the substrate, the enzyme was incubated in assay buffer (20 mM Hepes, 0.5 mM EDTA, pH 7.8, containing 0.1 mg/ml ovalbumin, and 5 mM dithiothreitol) for 2 h to prevent oxidation of thiol groups. The substrate was diluted with assay buffer to a final concentration of 17.6–900 nM and a 50-μl aliquot was added to each well on the 96-well plate. The assay was initiated by the addition of 50 μl of stock enzyme solution. Fluorescence ($\lambda_{ex} = 355$ nm, $\lambda_{em} = 460$ nm) of AMC was monitored continuously using a Wallac 1420 multi-label counter (Perkin–Elmer, Turk, Finland), and the concentration of AMC was determined using standard curves of fully digested substrates. Initial velocity data were used to determine K_m and k_{cat} values from nonlinear fits of the Michaelis–Menten equation.

Circular dichroism. Circular dichroism (CD) measurements were performed as described in [31]. Purified recombinant human UCH-L1 and mutants were adjusted to a concentration of 0.1 mg/ml and dialyzed against 20 mM sodium phosphate buffer (pH 8.0). Far UV CD spectra (195–250 nm) were recorded in a 1-mm quartz cuvette on a Jasco J-820 spectropolarimeter (Jasco, Tokyo, Japan) equipped with a temperature controller by scanning at the rate of 50 nm/min at 20 °C. For all spectra, six scans were averaged. All CD spectra were corrected by background

subtraction for the spectrum obtained with buffer alone and smoothed. The observed ellipticity was normalized to units of degrees-cm^2/dmol. The spectra were analyzed for percent secondary structural elements by a computer program based on an algorithm that compares experimental spectra with those of known proteins [32]. Student's t test was used to compare the significance of the differences between data.

Modification of human UCH-L1. Recombinant 6HN-tagged human UCH-L1 proteins (0.3 mg/ml) were incubated with various concentrations (0–1.0 mM) of HNE (Calbiochem, San Diego, CA) in 60 μl of 50 mM sodium phosphate buffer (pH 7.2) for 2 h at 37 °C, as described in [33]. HNE-modification of UCH-L1 was monitored by SDS–PAGE and immunoblotting. Modified proteins (500 ng) were dissolved in the SDS–PAGE sample buffer and separated by 10–20% gradient SDS–PAGE prior to transfer to a PVDF membrane (Bio-Rad, Hercules, CA). After blocking with 5% nonfat dried milk and 3% goat serum in PBS, blots were probed with rabbit anti-HNE Michael Adducts antibody (1:2000, Calbiochem). Following washes, proteins reacting with a secondary antibody, HRP-conjugated goat anti-rabbit IgG (1:2000, Dako), were visualized using SuperSignal West Femto Maximum Sensitivity Substrate (Pierce).

Assay of residual hydrolase activity. HNE modified sample (55 μl) was applied to a MicroSpin G-25 Column (Amersham Pharmacia Biotech) to separate protein-bound HNE from free HNE. Recovery of the protein was established by SDS–PAGE and staining with Coomassie brilliant blue R-250. Residual activity of the modified enzyme was determined as described above. Initial velocity data were used to determine the values for relative activity.

Results

Purification and characterization of recombinant human UCH-L1 proteins

To obtain wild-type UCH-L1 and the variants I93M and S18Y associated with Parkinson's disease (Fig. 1A), N-terminal 6HN-tagged recombinant proteins were expressed in *E. coli* and purified by metal chelate affinity

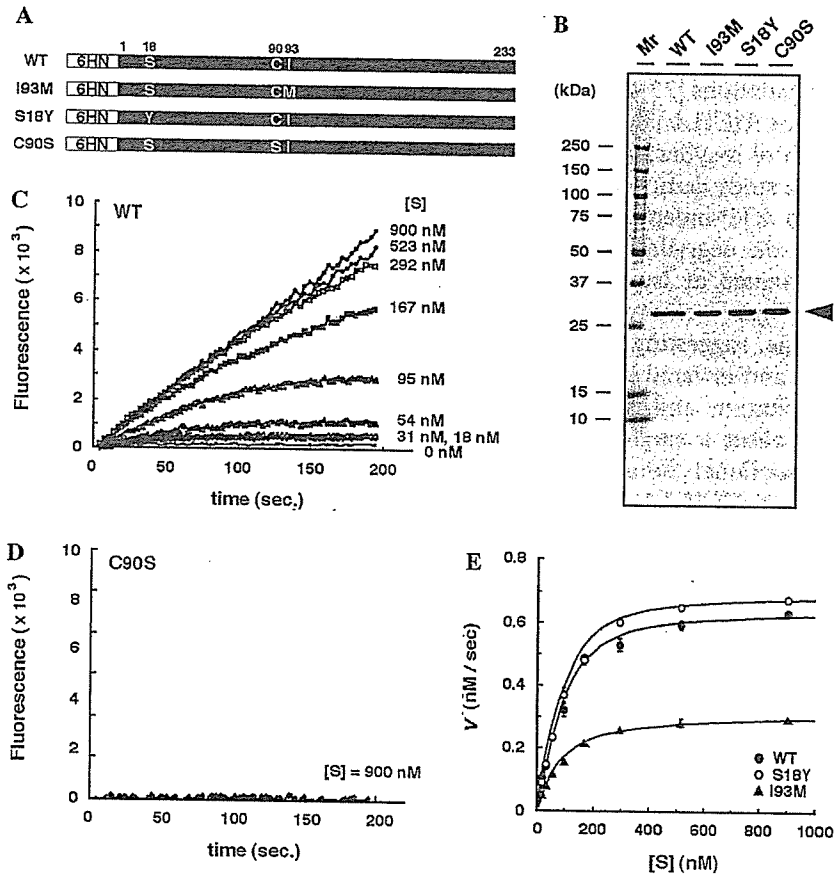

Fig. 1. Characterization and analysis of purified recombinant 6HN-tagged human UCH-L1s. (A) Schematic representation of 6HN-tagged human UCH-L1 wild-type (WT) and mutants I93M, S18Y, and C90S. The numbers indicate the amino acid residues of the N- and C-termini of UCH-L1 (open reading frame). The positions of the point mutations are indicated. The N-terminal 6HN-tag is shown in white. (B) Visualization of recombinant 6HN-tagged human UCH-L1s by SDS–PAGE under reducing conditions and Coomassie staining. One microgram of each sample was subjected to analysis. The *arrow* indicates the 28.9-kDa 6HN-tagged human UCH-L1 bands. M_r, molecular weight markers (kDa). (C) Kinetics of WT UCH-L1-catalyzed hydrolysis of Ub-AMC. Fluorescence intensity ($\lambda_{ex} = 355$ nm, $\lambda_{em} = 460$ nm) is indicated as a function of time. Enzyme concentration was 4.3 nM and substrate concentrations are indicated on the right. (D) Kinetics of C90S UCH-L1-catalyzed hydrolysis of Ub-AMC. Enzyme concentration was 4.3 μM and substrate concentration was 900 nM. (E) Effect of Ub-AMC concentration on the initial velocity of hydrolysis for WT UCH-L1 and variants. Activity measurements were performed using 4.3 nM 6HN-tagged human UCH-L1 or variant. Closed circle, WT; open circle, S18Y; closed triangle, I93M. Each value represents the mean ± SE of three independent experiments. Error bars are not shown if the error is smaller than the symbol.

chromatography. Coomassie staining of the purified proteins following SDS–PAGE showed a single 28.9-kDa band for each of the 6HN-tagged proteins (Fig. 1B) in good agreement with the theoretical 27.8-kDa molecular mass of the 6HN-tagged UCH-L1. The expression levels for the wild-type and variant UCH-L1 proteins were equivalent. As a negative control, we prepared a recombinant human C90S UCH-L1 in which serine is substituted within the active center triad [11] (Fig. 1A). The purified C90S UCH-L1 exhibited no hydrolase activity even at a very high concentration of 5 μM (Table 1; Fig. 1D), supporting the SDS–PAGE result (Fig. 1B) that there were no contaminant proteins with hydrolase activity in our recombinant protein preparations.

Kinetics of Ub-AMC hydrolysis by wild-type and variant UCH-L1s

UCH-L1 is a ubiquitin hydrolase that specifically cleaves small adducts of C-terminally modified ubiquitin (ubiquitin$^{1-72}$-Leu^{73}-Arg^{74}-Gly^{75}-Gly^{76}-X, where X can be any leaving group such as an amine, thiol group, small peptide, and polypeptide) [12]. To determine the enzymatic activities of recombinant human UCH-L1 and variants, we performed a general deubiquitinating assay using Ub-AMC as a substrate. Ub-AMC is efficiently hydrolyzed by UCH-L3 to liberate the highly fluorescent AMC moiety [30]. The hydrolase activity of wild-type UCH-L1 was compared with those of the parkinsonism-associated variants. Using varying concentrations of Ub-AMC, a Michaelis–Menten saturation curve was generated to determine the kinetics of catalysis for wild-type human UCH-L1 (Fig. 1C). Catalysis was saturated at 600–900 nM Ub-AMC (Figs. 1C and E). Next, steady-state kinetic parameters for each UCH-L1 mutant were determined using 4.3 nM wild-type and variant UCH-L1 and varying concentrations of Ub-AMC. The initial velocities were fit to the Michaelis–Menten equation to provide nonlinear least-squares parameters (Fig. 1E; Table 1). The k_{cat} for the wild-type UCH-L1 was 0.174 ± 0.0057 s^{-1}, while k_{cat} for the I93M and S18Y variants was 0.0794 ± 0.0034 s^{-1} and 0.196 ± 0.0028 s^{-1}, respectively (wild-type vs I93M, $p < 0.01$; wild-type vs S18Y, $p < 0.05$). The hydrolase activity of the I93M mutant was 45.6% of that of the wild-type UCH-L1. In contrast, the activity of the S18Y UCH-L1 variant was 1.13-fold higher than that of wild-type. The mutant and wild-type proteins exhibited similar K_m values, $K_m^{wt} = (122 \pm 10) \times 10^{-9}$ M, $K_m^{I93M} = (110 \pm 14) \times 10^{-9}$ M, and $K_m^{S18Y} = (136 \pm 1.7) \times 10^{-9}$ M, indicating that the mutant proteins showed similar affinity for Ub-AMC. In another study using recombinant UCH-L1, Liu et al. [29] reported that the S18Y and wild-type proteins exhibit equivalent hydrolase activities. The disagreement between their results and ours may be due to differences in protein preparations and/or hydrolase assay methods. We confirmed that the difference in the hydrolase activities of wild-type and S18Y UCH-L1s was statistically significant using independent protein preparations, and therefore we are confident that the hydrolase activity of S18Y UCH-L1 is higher than that of wild-type UCH-L1. The increased hydrolase activity appears to be a direct result of the S18Y mutation since the S18Y and wild-type UCH-L1 preparations contain no contaminant proteins or activities (Figs. 1B–D). Also, both proteins exhibit the same CD spectra (Fig. 2A). Significantly, the increased hydrolase activity of S18Y UCH-L1 was recently confirmed by another group [34].

Table 1
Kinetic parameters for hydrolysis of Ub-AMC by human UCH-L1s

Enzyme	k_{cat} (s^{-1})	K_m (nM)
UCH-L1 (wild-type)	0.174 ± 0.0057	122 ± 10
I93M	$0.0794^{**} \pm 0.0034$	110 ± 14
S18Y	$0.196^{*} \pm 0.0028$	136 ± 1.7
C90S[a]	N.D.[b]	N.D.[b]

Each value represents the means ± SE from three independent sets of experiments. $^{*}p < 0.05$, $^{**}p < 0.01$ compared with values for UCH-L1 (wild-type) by t test.

[a] No hydrolyzed products were observed after 1 h with 5 μM enzyme.

[b] N.D., not detectable.

CD analysis of secondary structure in wild-type and variant human UCH-L1s

To address whether the observed differences in hydrolase activities of the variant UCH-L1s reflect altered secondary structure, we utilized CD spectroscopy to estimate secondary structure in the recombinant proteins (Fig. 2A). Human UCH-L1 and the variant proteins exhibited spectra with distinct minima at 208 and 222 nm, characteristic of high α-helical content (Fig. 2A). The ratios of α-helix, β-sheet, and other secondary structural features in these proteins were estimated from mean residue ellipticity data and are presented graphically in Fig. 2B. Relative to wild-type, the I93M mutant displayed slightly lower ellipticity over the range 195–200 nm, indicating decreased α-helical content (Fig. 2A, left). As a control, we prepared a recombinant double mutant UCH-L1 containing both the S18Y and I93M substitutions. The CD spectrum of the S18Y–I93M double mutant over 195–200 nm was similar to that of I93M (Fig. 2A, right), indicating that the amino acid substitution at position 93 is responsible for the decreased α-helical content. In contrast, the CD spectrum of the S18Y variant exhibited no difference compared to that of the wild-type protein.

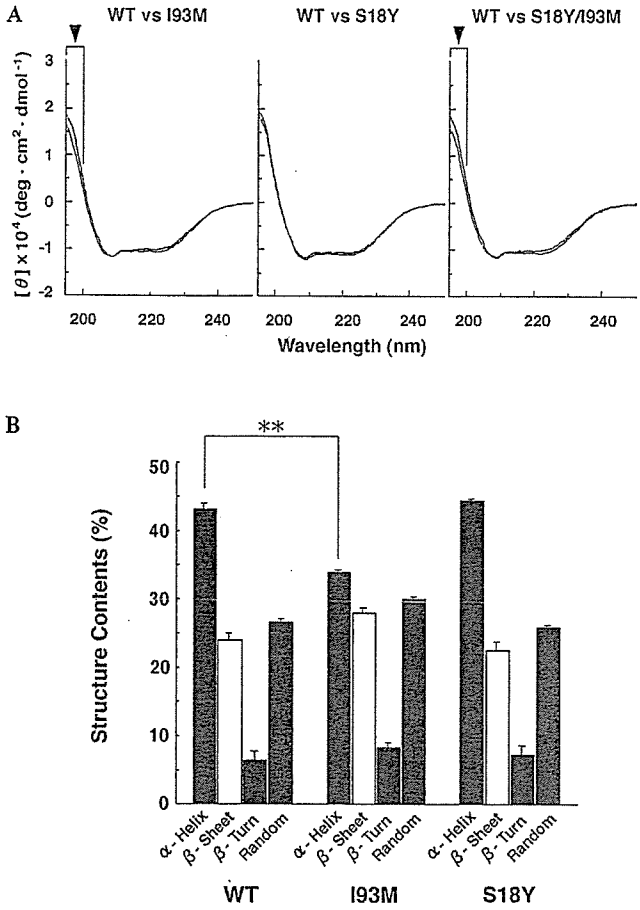

Fig. 2. CD spectra and secondary structural content of 6HN-tagged human UCH-L1s. (A) CD spectra (mean residue ellipticity) for recombinant proteins (0.1 mg/ml) in 50 mM sodium phosphate buffer. Wild-type UCH-L1 (WT) is shown in blue, I93M in green, S18Y in red, and S18Y-I93M in violet. Six scans were averaged for all spectra. *Arrowheads* indicate the differences of CD spectra. (B) Secondary structural content of recombinant human 6HN-tagged UCH-L1s. Each value represents the mean ± SE of six data sets. *p* value (*t* test) for the WT vs other proteins: **, < 0.01.

Modification and inactivation of UCH-L1 hydrolase activity by HNE

UCH-L1 belongs to a papain-like cysteine protease family [4,35] with conserved Cys and His residues within the active site. Certain cysteine proteases are known to be targets of cellular oxidative stress [36], and several lines of evidence implicate this phenomenon in sporadic PD [46]. One of the endogenous factors that is toxic to neurons during oxidative stress is HNE, an aldehyde product of fatty acid peroxidation. HNE can induce neuronal death [37,38] and is thought to form covalent cross-links with proteins via Michael addition to Cys, His, and Lys residues, thus altering the function of cysteine proteases [36]. HNE-modified proteins have been detected in nigral neurons and Lewy bodies in sporadic PD [39,40]. We examined whether HNE directly modifies/inactivates UCH-L1 in vitro. Past studies determined that HNE is produced in micromolar concentrations in response to certain oxidative stresses [41–43]. We utilized micromolar concentrations of HNE and 10 μM UCH-L1 for our experiments (UCH-L1 is an abundant protein, comprising 1–2% of soluble brain protein) [17,44]. Physiological concentrations of HNE (10–100 μM) were sufficient to covalently modify UCH-L1 and reduce hydrolase activity by 40–80% (Figs. 3A and B). Covalent modification also occurred at a lower

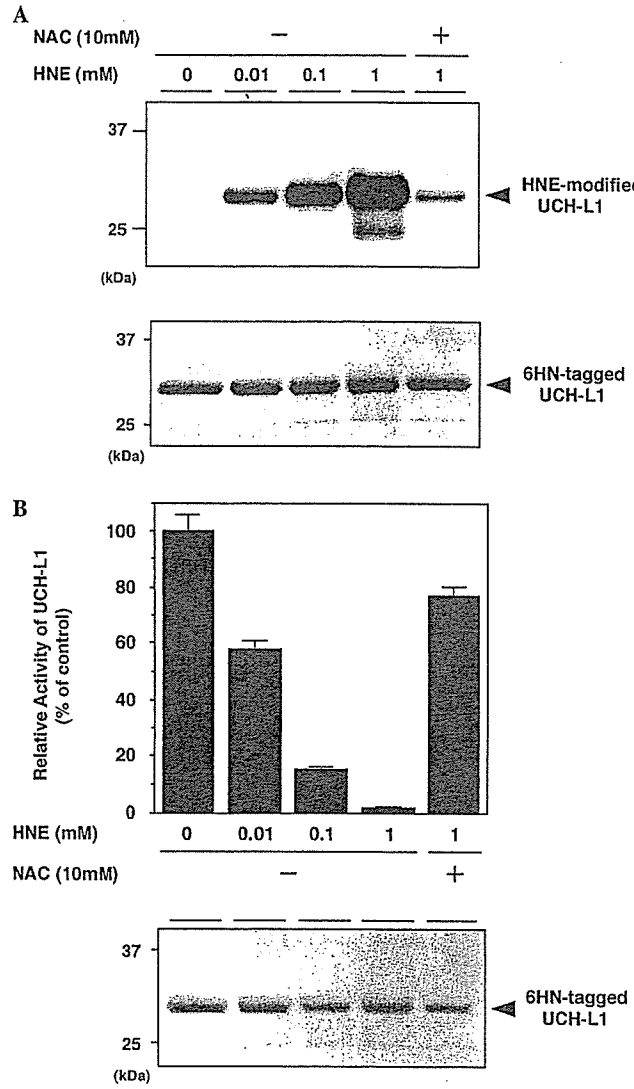

Fig. 3. Effect of HNE and NAC on UCH-L1 hydrolase activity. (A) Modification of wild-type UCH-L1 with HNE was visualized by immunoblot analysis with HNE adduct-specific antibody (top panel). HNE-modified UCH-L1 from the same sample was resolved by SDS–PAGE and stained with Coomassie brilliant blue (bottom panel). (B) Inactivation of UCH-L1 hydrolase activity by HNE and rescue with NAC (top panel). The residual activities of HNE-modified UCH-L1 prepared from the same sample shown in (A) were measured by hydrolase assay. Each value represents the mean ± SE of four experiments. The HNE-modified UCH-L1 proteins were separated from free HNE, resolved by SDS–PAGE, and stained with Coomassie brilliant blue (bottom panel).

concentration of UCH-L1 (1.25 μM; data not shown). Moreover, excess *N*-acetyl-L-cysteine (NAC: as a competitive cysteine analogue) prevented both HNE modification (Fig. 3A) and the decrease in hydrolase activity, thus confirming that human UCH-L1 was modified with HNE (Fig. 3B).

Discussion

We analyzed the hydrolase activities of parkinsonism-associated UCH-L1 variants, I93M and S18Y. The I93M mutation causes a decrease in the hydrolase activity in agreement with a previous report [19]. Furthermore, the S18Y variant exhibits slightly higher hydrolase activity than the wild-type enzyme. We also examined the structural features of the UCH-L1 variants by CD spectroscopy. The wild-type and S18Y UCH-L1 proteins elicit essentially identical CD spectra while the I93M mutant exhibits a decrease in α-helical content. Finally, we found that UCH-L1 modification by HNE decreases its hydrolase activity.

The I93M UCH-L1 mutant exhibits reduced hydrolase activity (~55% of wild-type), and this mutant displays 80% penetrance in a German family carrying the allele [19]. Conversely, genetic-epidemiological studies demonstrated that carriers of the S18Y UCH-L1 polymorphism that causes increased hydrolase activity show a decreased risk of sporadic PD. Furthermore, the risk of PD is also dependent on the S18Y allele dosage in that homozygotes of this allele are at lower relative risk (0.31) than heterozygotes (relative risk between 0.55 and 0.81) [21,24,25]. Thus, the PD risk appears to correlate inversely with the hydrolase activity of the UCH-L1 variants associated with PD (Table 2), suggesting that increased hydrolase activity may confer protection against the development of PD while decreased activity may be involved in PD pathogenesis.

Another study using recombinant UCH-L1 proteins demonstrated that UCH-L1 has dual enzymatic activity, both as a ubiquitin hydrolase and an ATP-independent ubiquitin ligase for α-synuclein [29]. It was also shown that the ligase activity of S18Y UCH-L1 is decreased relative to that of the wild-type UCH-L1. These results suggest that the ligase activity, in addition to the hydrolase activity, is involved in PD etiology. Our results demonstrate that the I93M mutation both impairs hydrolase activity and perturbs the structure in the protein. Given that UCH-L1 is an abundant protein (1–2% of soluble brain protein) [17] and constitutes a principal component of Lewy bodies in sporadic PD [45], such a structural alteration may contribute to the accumulation/aggregation of UCH-L1 (and/or mutants thereof) in the diseased state. Thus, there may be a correlation between structural changes within UCH-L1 and PD-associated Lewy body formation. However, further detailed biochemical and biophysical characterization of the I93M UCH-L1 mutant is required to confirm this possibility.

The protein structure is altered only in I93M UCH-L1 and the ligase activity is decreased both in I93M and S18Y UCH-L1s [29]. However, only the hydrolase activity correlates inversely with the risk of PD (Table 2). Therefore, the change in hydrolase activity in both I93M and S18Y UCH-L1 variants may be responsible, in whole or part, for the differences in PD risk observed in the two populations carrying these distinct alleles.

Two other causative genes, *parkin* and *α-synuclein*, have been linked to familial PD (reviewed in 46). Parkin exhibits E3 ubiquitin ligase activity [47,48]. Parkin-associated endothelin receptor-like receptor (Pael-R) has been identified as a substrate for parkin [49]. Parkin is thought to remove misfolded proteins such as Pael-R from the endoplasmic reticulum (ER) and to protect neurons from ER-mediated stress-induced cell death [49]. α-Synuclein, a core component of Lewy bodies [50], is also a substrate for parkin and therefore parkin may be involved in Lewy body formation as well [51]. It was proposed that UCH-L1 is a neuron-specific ubiquitin hydrolase required to maintain cellular levels of 'free ubiquitin' (i.e., ligatable at the C-terminus) [12]. The decreased hydrolase activity of the I93M UCH-L1 mutant possibly results in reduced levels of free ubiquitin that may adversely affect the normal degradation of Pael-R and α-synuclein. Conversely, the increased hydrolase activity of the S18Y mutant may elevate cellular free ubiquitin levels, resulting in enhanced degradation of Pael-R and α-synuclein. Moreover, the increased hydrolase activity of S18Y UCH-L1 coupled with its decreased ligase activity (which can prevent α-synuclein degradation by K63-linked ubiquitin ligation) [29] may be additive or synergistic with respect to the decreased risk of sporadic PD. These hypotheses may be confirmed in future in vivo studies designed to measure cellular

Table 2
Association between Parkinson's disease and human UCH-L1 mutants

UCH-L1 variant	WT	I93M	S18Y	References
Incidence of Parkinson's disease		↑	↓	[19–24]
Hydrolase activity	(100%)	↓ (45.6%)	↑ (112.6%)	[19, this study]
CD spectra alteration	Normal	↓ (α-Helix)	Normal	
Ubiquitin ligase activity	(100%)	↓	↓↓	[29]

levels of C-terminal-modified and -free ubiquitin in nigral neurons expressing PD-associated UCH-L1 variants.

Oxidative stress is believed to play a role in the pathogenesis of sporadic PD by promoting the generation and accumulation of oxidant-modified proteins that exhibit aberrant properties [46,52]. HNE, a good candidate for an endogenous toxic oxidizing factor, possibly affects the neuronal ubiquitin–proteasome pathway since UCH-L1 is directly modified by HNE in vitro, resulting in a significant decrease in hydrolase activity. This loss of activity could affect the level of free ubiquitin in a manner similar to that of the UCH-L1 mutants, and consequently may affect the risk of PD. Therefore, the disruption of control mechanisms within the ubiquitin–proteasome pathway via changes in UCH-L1 hydrolase activity may represent a common origin for the pathogenesis of both sporadic and familial PD.

Acknowledgments

This work was supported in part by Grants-in-Aid for Scientific Research from the Ministry of Health, Labour and Welfare of Japan, Grants-in-Aid for Scientific Research from the Ministry of Education, Culture, Sports, Science and Technology of Japan, a grant from the Organization for Pharmaceutical Safety and Research, a grant from Japan Science and Technology Cooperation, and a grant from the Japan Society for the Promotion of Science (JSPS) Research Fellowships (to S.A.). Y.-L.W. is a research fellowship of the Japan Foundation for Aging and Health.

References

[1] K.D. Wilkinson, Ubiquitin-dependent signaling: the role of ubiquitination in the response of cells to their environment, J. Nutr. 129 (1999) 1933–1936.
[2] A. Hershko, A. Ciechanover, The ubiquitin system, Annu. Rev. Biochem. 67 (1998) 425–479.
[3] A. Ciechanover, A. Orian, A.L. Schwartz, The ubiquitin-mediated proteolytic pathway: mode of action and clinical implications, J. Cell Biochem. Suppl. 34 (2000) 40–51.
[4] K.D. Wilkinson, Regulation of ubiquitin-dependent processes by deubiquitinating enzymes, FASEB J. 11 (1997) 1245–1256.
[5] K.D. Wilkinson, M. Hochstrasser, The deubiquitinating enzyme, in: J.M. Peters, J.R. Harris, D. Finley (Eds.), Ubiquitin and the Biology of the Cell, Plenum Press, New York, 1998, pp. 99–125.
[6] R.T. Baker, J.W. Tobias, A. Varshavsky, Ubiquitin-specific proteases of *Saccharomyces cerevisiae*. Cloning of UBP2 and UBP3, and functional analysis of the UBP gene family, J. Biol. Chem. 267 (1992) 23364–23375.
[7] M. Hochstrasser, Protein degradation or regulation: Ub the judge, Cell 84 (1996) 813–815.
[8] C.M. Pickart, I.A. Rose, Ubiquitin carboxyl-terminal hydrolase acts on ubiquitin carboxyl-terminal amides, J. Biol. Chem. 260 (1985) 7903–7910.
[9] J.W. Tobias, A. Varshavsky, Cloning and functional analysis of the ubiquitin-specific protease gene UBP1 of *Saccharomyces cerevisiae*, J. Biol. Chem. 266 (1991) 12021–12028.
[10] M.J. Schlesinger, U. Bond, Ubiquitin genes, Oxf. Surv. Eukaryot Genes 4 (1987) 77–91.
[11] C.N. Larsen, J.S. Price, K.D. Wilkinson, Substrate binding and catalysis by ubiquitin C-terminal hydrolases: identification of two active site residues, Biochemistry 35 (1996) 6735–6744.
[12] C.N. Larsen, B.A. Krantz, K.D. Wilkinson, Substrate specificity of deubiquitinating enzymes: ubiquitin C-terminal hydrolases, Biochemistry 37 (1998) 3358–3368.
[13] A.N. Mayer, K.D. Wilkinson, Detection, resolution, and nomenclature of multiple ubiquitin carboxyl- terminal esterases from bovine calf thymus, Biochemistry 28 (1989) 166–172.
[14] K.D. Wilkinson, Roles of ubiquitinylation in proteolysis and cellular regulation, Annu. Rev. Nutr. 15 (1995) 161–189.
[15] Y. Osawa, Y.L. Wang, H. Osaka, S. Aoki, K. Wada, Cloning, expression, and mapping of a mouse gene, Uchl4, highly homologous to human and mouse Uchl3, Biochem. Biophys. Res. Commun. 283 (2001) 363–627.
[16] K.D. Wilkinson, S. Deshpande, C.N. Larsen, Biochem. Comparisons of neuronal (PGP 9.5) and non-neuronal ubiquitin C-terminal hydrolases, Soc. Trans. 20 (1992) 631–637.
[17] K.D. Wilkinson, K.M. Lee, S. Deshpande, P. Duerksen-Hughes, J.M. Boss, J. Pohl, The neuron-specific protein PGP 9.5 is a ubiquitin carboxyl-terminal hydrolase, Science 246 (1989) 670–673.
[18] K. Saigoh, Y.L. Wang, J.G. Suh, T. Yamanishi, Y. Sakai, H. Kiyosawa, T. Harada, N. Ichihara, S. Wakana, T. Kikuchi, K. Wada, Intragenic deletion in the gene encoding ubiquitin carboxy-terminal hydrolase in gad mice, Nat. Genet. 23 (1999) 47–51.
[19] E. Leroy, R. Boyer, G. Auburger, B. Leube, G. Ulm, E. Mezey, G. Harta, M.J. Brownstein, S. Jonnalagada, T. Chernova, A. Dehejia, C. Lavedan, T. Gasser, P.J. Steinbach, K.D. Wilkinson, M.H. Polymeropoulos, The ubiquitin pathway in Parkinson's disease, Nature 395 (1998) 451–452.
[20] Y. Momose, M. Murata, K. Kobayashi, M. Tachikawa, Y. Nakabayashi, I. Kanazawa, T. Toda, Association studies of multiple candidate genes for Parkinson's disease using single nucleotide polymorphisms, Ann. Neurol. 51 (2002) 133–136.
[21] J. Satoh, Y. Kuroda, A polymorphic variation of serine to tyrosine at codon 18 in the ubiquitin C-terminal hydrolase-L1 gene is associated with a reduced risk of sporadic Parkinson's disease in a Japanese population, J. Neurol. Sci. 189 (2001) 113–117.
[22] P. Wintermeyer, R. Kruger, W. Kuhn, T. Muller, D. Woitalla, D. Berg, G. Becker, E. Leroy, M. Polymeropoulos, K. Berger, H. Przuntek, L. Schols, J.T. Epplen, O. Riess, Mutation analysis and association studies of the UCHL1 gene in German Parkinson's disease patients, Neuroreport 11 (2000) 2079–2082.
[23] J. Zhang, N. Hattori, E. Leroy, H.R. Morris, S. Kubo, T. Kobayashi, N.W. Wood, M.H. Polymeropoulos, Y. Mizuno, Association between a polymorphism of ubiquitin carboxy-terminal hydrolase L1 (UCH-L1) gene and sporadic Parkinson's disease, Parkinsonism Relat. Disord. 6 (2000) 195–197.
[24] D.M. Maraganore, M.J. Farrer, J.A. Hardy, S.J. Lincoln, S.K. McDonnell, W.A. Rocca, Case-control study of the ubiquitin carboxy-terminal hydrolase L1 gene in Parkinson's disease, Neurology 53 (1999) 1858–1860.
[25] C. Levecque, A. Destee, V. Mouroux, E. Becquet, L. Defebvre, P. Amouyel, M.C. Chartier-Harlin, No genetic association of the ubiquitin carboxy-terminal hydrolase-L1 gene S18Y polymorphism with familial Parkinson's disease, J. Neural Transm. 108 (2001) 979–984.
[26] G. Savettieri, E.V. De Marco, D. Civitelli, G. Salemi, G. Nicoletti, G. Annesi, I.C. Ciro Candiano, A. Quattrone, Lack of association between ubiquitin carboxy-terminal hydrolase L1 gene polymorphism and PD, Neurology 57 (2001) 560–561.
[27] G.D. Mellick, P.A. Silburn, The ubiquitin carboxy-terminal hydrolase-L1 gene S18Y polymorphism does not confer protection against idiopathic Parkinson's disease, Neurosci. Lett. 293 (2000) 127–130.

[28] S. Lincoln, J. Vaughan, N. Wood, M. Baker, J. Adamson, K. Gwinn-Hardy, T. Lynch, J. Hardy, M. Farrer, Low frequency of pathogenic mutations in the ubiquitin carboxy-terminal hydrolase gene in familial Parkinson's disease, Neuroreport 10 (1999) 427–429.

[29] Y. Liu, L. Fallon, H.A. Lashuel, Z. Liu, P.T. Lansbury Jr., The UCH-L1 gene encodes two opposing enzymatic activities that affect α-synuclein degradation and Parkinson's disease susceptibility, Cell 111 (2002) 209–218.

[30] L.C. Dang, F.D. Melandri, R.L. Stein, Kinetic and mechanistic studies on the hydrolysis of ubiquitin C- terminal 7-amido-4-methylcoumarin by deubiquitinating enzymes, Biochemistry 37 (1998) 1868–1879.

[31] R.J. Perrin, W.S. Woods, D.F. Clayton, J.M. George, Interaction of human α-synuclein and Parkinson's disease variants with phospholipids. Structural analysis using site-directed mutagenesis, J. Biol. Chem. 275 (2000) 34393–34398.

[32] J.T. Yang, C.S. Wu, H.M. Martinez, Calculation of protein conformation from circular dichroism, Methods Enzymol. 130 (1986) 208–269.

[33] K. Uchida, E.R. Stadtman, Covalent attachment of 4-hydroxynonenal to glyceraldehyde-3-phosphate dehydrogenase. A possible involvement of intra- and intermolecular cross-linking reaction, J. Biol. Chem. 268 (1993) 6388–6393.

[34] P.J. Lockhart, L. Hill, T. Chernova, K. Wilkinson, M.J. Farrer, in: Proceedings of the 32th Annual Meeting Society for Neuroscience, Orlando, FL, November 2–7, 2002 (Abstr. 887.6), Society for neuroscience, Washington, DC, 2002.

[35] S.C. Johnston, C.N. Larsen, W.J. Cook, K.D. Wilkinson, C.P. Hill, Crystal structure of a deubiquitinating enzyme human (UCH-L3) at 1.8A resolution, EMBO J. 16 (1997) 3787–3796.

[36] J.W. Crabb, J. O'Neil, M. Miyagi, K. West, H.F. Hoff, Hydroxynonenal inactivates cathepsin B by forming Michael adducts with active site residues, Protein Sci. 11 (2002) 831–840.

[37] J.N. Keller, K.B. Hanni, W.R. Markesbery, 4-hydroxynonenal increases neuronal susceptibility to oxidative stress, J. Neurosci. Res. 58 (1999) 823–830.

[38] I. Kruman, A.J. Bruce-Keller, D. Bredesen, G. Waeg, M.P. Mattson, Evidence that 4-hydroxynonenal mediates oxidative stress-induced neuronal apoptosis, J. Neurosci. 17 (1997) 5089–5100.

[39] A. Yoritaka, N. Hattori, K. Uchida, M. Tanaka, E.R. Stadtman, Y. Mizuno, Immunohistochemical detection of 4-hydroxynonenal protein adducts in Parkinson disease, Proc. Natl. Acad. Sci. USA 93 (1996) 2696–2701.

[40] R.J. Castellani, G. Perry, S.L. Siedlak, A. Nunomura, S. Shimohama, J. Zhang, T. Montine, L.M. Sayre, M.A. Smith, Hydroxynonenal adducts indicate a role for lipid peroxidation in neocortical and brainstem Lewy bodies in humans, Neurosci. Lett. 319 (2002) 25–28.

[41] H. Esterbauer, R.J. Schaur, H. Zollner, Chemistry and biochemistry of 4-hydroxynonenal, malonaldehyde and related aldehydes, Free Radic. Biol. Med. 11 (1991) 81–128.

[42] A.M. Gioacchini, N. Calonghi, C. Boga, C. Cappadone, L. Masotti, A. Roda, P. Traldi, Determination of 4-hydroxy-2-nonenal at cellular levels by means of electrospray mass spectrometry, Rapid. Commun. Mass Spectrom 13 (1999) 1573–1579.

[43] M.L. Selley, (E)-4-hydroxy-2-nonenal may be involved in the pathogenesis of Parkinson's disease, Free Radic. Biol. Med. 25 (1998) 169–174.

[44] J.F. Doran, P. Jackson, P.A. Kynoch, R.J. Thompson, Isolation of PGP 9.5, a new human neurone-specific protein detected by high-resolution two-dimensional electrophoresis, J. Neurochem. 40 (1983) 1542–1547.

[45] J. Lowe, H. McDermott, M. Landon, R.J. Mayer, K.D. Wilkinson, Ubiquitin carboxyl-terminal hydrolase (PGP 9.5) is selectively present in ubiquitinated inclusion bodies characteristic of human neurodegenerative diseases, J. Pathol. 161 (1990) 153–160.

[46] M.M. Mouradian, Recent advances in the genetics and pathogenesis of Parkinson disease, Neurology 58 (2002) 179–185.

[47] H. Shimura, N. Hattori, S. Kubo, Y. Mizuno, S. Asakawa, S. Minoshima, N. Shimizu, K. Iwai, T. Chiba, K. Tanaka, T. Suzuki, Familial Parkinson disease gene product, parkin, is a ubiquitin–protein ligase, Nat. Genet. 25 (2000) 302–305.

[48] Y. Zhang, J. Gao, K.K. Chung, H. Huang, V.L. Dawson, T.M. Dawson, Parkin functions as an E2-dependent ubiquitin- protein ligase and promotes the degradation of the synaptic vesicle-associated protein, CDCrel-1, Proc. Natl. Acad. Sci. USA 97 (2000) 13354–13359.

[49] Y. Imai, M. Soda, H. Inoue, N. Hattori, Y. Mizuno, R. Takahashi, An unfolded putative transmembrane polypeptide, which can lead to endoplasmic reticulum stress, is a substrate of Parkin, Cell 105 (2001) 891–902.

[50] M.G. Spillantini, M.L. Schmidt, V.M. Lee, J.Q. Trojanowski, R. Jakes, M. Goedert, α-Synuclein in Lewy bodies, Nature 388 (1997) 839–840.

[51] H. Shimura, N. Hattori, S. Kubo, M. Yoshikawa, T. Kitada, H. Matsumine, S. Asakawa, S. Minoshima, Y. Yamamura, N. Shimizu, Y. Mizuno, Immunohistochemical and subcellular localization of Parkin protein: absence of protein in autosomal recessive juvenile parkinsonism patients, Ann. Neurol. 45 (1999) 668–672.

[52] E.R. Stadtman, R.L. Levine, Protein oxidation, Ann. N. Y. Acad. Sci. 899 (2000) 191–208.

Absence of Association between Codon 129/219 Polymorphisms of the Prion Protein Gene and Alzheimer's Disease in Japan

Takuya Ohkubo, MD,[1,2] Yuji Sakasegawa, MSc,[1]
Takashi Asada, MD,[3] Toru Kinoshita, MD,[4]
Yuichi Goto, MD, PhD,[4] Hideo Kimura, PhD,[5]
Hidehiro Mizusawa, MD, PhD,[2]
Naomi S. Hachiya, PhD,[1,6]
and Kiyotoshi Kaneko, MD, PhD[1,6]

Alzheimer's disease (AD) might share a common pathogenic mechanism, in terms of conformation disorders, with prion disease such as Creutzfeldt–Jakob disease (CJD), which is characterized by the accumulation of abnormally folded prion protein in the brain.[1] Although it has been reported that codon 129 polymorphism (either methionine [M] or valine [V]) of the prion protein (*PRNP*) gene might be a risk factor for Alzheimer's disease (AD) in some European populations (French and Dutch),[2,3] it was not confirmed by two studies in Italian and Spanish populations.[4,5] With this background, we examined whether codon 129 polymorphism of the *PRNP* gene confers susceptibility to AD in nonwhite population. Furthermore, we also examined another polymorphism (either glutamate [E] or lysine [K]) at codon 219 of the *PRNP* gene, which is confined to Japanese population so far and known to render humans resistant to sporadic CJD.[6]

Five hundred forty-eight Japanese patients with probable AD (191 men and 357 women; mean age of onset, 70.4 ± 9.0 years old), whose diagnoses were determined by meeting the National Institute of Neurological and Communicative Disorders and Stroke and the Alzheimer's Disease and Related Dementias Association criteria, and 466 healthy controls (206 men and 260 women; mean age, 67.7 ±10.0 years old) were analyzed. The 1.02kb region harboring the entire open reading frame of the *PRNP* gene was sequenced in all subjects, but no novel polymorphism was detected other than two known polymorphisms at codon 129 and 219.[6] The expected difference in the apolipoprotein E (APOE) ε4 allele frequency, which is known as a major risk factor in cognitive dementia,[7] was observed between AD patients and control subjects (odds ratio, 2.93; 95% confidence interval, 2.23–3.85), suggesting that there was no apparent population bias in our study.

Genotypic analysis of codon 129 of the *PRNP* gene (Table) showed no association with Japanese AD (n = 548/466 [AD/control]; $p = 0.90$); early-onset AD (EOAD; age of onset, <65 years; n = 136/156; $p = 0.54$); or late-onset AD (LOAD; age of onset, ≥ 65 years; n = 412/310; $p = 0.77$), regardless of their APOE ε4 statuses (data not shown). Next, we also studied another *PRNP* gene polymorphism at codon 219 (see Table), which is confined to a Japanese population so far examined and renders resistance to sporadic CJD.[6] Again, no association was shown between codon 219 polymorphism and Japanese AD (n = 548/466; $p = 0.88$); EOAD (n = 136/156; $p = 0.54$); or LOAD (n = 412/310; $p = 0.65$), regardless of their APOE ε4 statuses (data not shown). Finally, we performed haplotype analysis that would increase informativeness as a genetic marker,[8] because the codon 129 and 219 polymorphisms are not sufficiently informative. As a result, it showed no association between heterozygosity of codon 129/219 of the PRNP gene and Japanese AD (total AD; $p = 0.99$, EOAD; $p = 0.84$, LOAD; $p = 0.94$).

Combarros and colleagues[4] reported that the discrepancy between their negative study in a Spanish population and two other positive studies in Europeans[2,3] might reside in the different age distribution. Apparently, this is not the case in our study because the statistical analysis showed no difference of the age distribution. Casadei and colleagues[5] also reported the similar negative result in an Italian population, but they also suggested EOAD patients have a tendency of carrying at least one V allele at codon 129. In fact, prevalence of AD among Japanese is comparable with that among whites,[9] which might not support the association between valine at codon 129 and AD.

Table. Allele and Genotype Frequencies of Codon 129 and 219 Polymorphisms of the PRNP *Gene in Japanese AD Patients and Control Subject*

Subject Group	n	Genotype, n (%)			Allele Frequency	
		MM	MV	VV	M	V
Subjects with AD						
<65 yr	136	130 (95.6)	6 (4.4)	0 (0.0)	0.978	0.022
≥65 yr	412	381 (92.5)	31 (7.5)	0 (0.0)	0.962	0.038
Total	548	511 (93.2)	37 (6.8)	0 (0.0)	0.966	0.034
Control subjects						
<65 yr	156	147 (94.2)	9 (5.8)	0 (0.0)	0.971	0.029
≥65 yr	310	289 (93.2)	21 (6.8)	0 (0.0)	0.966	0.034
Total	466	436 (93.6)	30 (6.4)	0 (0.0)	0.968	0.032

Subject Group	n	Genotype, n (%)			Allele Frequency	
		EE	EK	KK	E	K
Subjects with AD						
<65 yr	136	108 (79.4)	27 (19.9)	1 (0.7)	0.893	0.107
≥65 yr	412	364 (88.3)	48 (11.7)	0 (0.0)	0.938	0.062
Total	548	472 (86.1)	75 (13.7)	1 (0.2)	0.930	0.070
Control subjects						
<65 yr	156	129 (82.7)	27 (17.3)	0 (0.0)	0.913	0.087
≥65 yr	310	270 (87.1)	40 (12.9)	0 (0.0)	0.935	0.065
Total	466	399 (85.6)	67 (14.4)	0 (0.0)	0.928	0.072

AD = Alzheimer's disease; EOAD = early-onset AD; LOAD = late-onset AD.

Our data are the first genetic association study of the *PRNP* gene with AD in nonwhite population. Of note, we examined a unique polymorphism at codon 219 in more than 1,000 Japanese patients with AD and age-matched controls. In addition, the haplotype analysis with codon 129/219 polymorphisms also was performed. Although our data demonstrated no association at present, further studies in different ethnic groups with more informative genetic markers, if any, have yet to be done to conclude such association between AD and the *PRNP* gene polymorphisms.

We thank N. Minami for providing the DNA samples of patients. This work was supported by a grant from the Program for Promotion of Fundamental Studies in Health Sciences and the Organization for Pharmaceutical Safety and Research, and Core Research for Evolutional Science and Technology (CREST) of Japan Science and Technology Corporation.

[1]Department of Cortical Function Disorders, National Institute of Neuroscience (NIN), National Center of Neurology and Psychiatry (NCNP), Tokyo; [2]Department of Neurology and Neurological Science, Graduate School of Medicine, Tokyo Medical and Dental University; [3]Department of Neuropsychiatry, Institute of Clinical Medicine, University of Tsukuba; [4]Department of Mental Retardation and Birth Defect Research; [5] Department of Molecular Genetics, NIN, NCNP, Tokyo; and [6]Core Research for Evolutional Science and Technology (CREST), Japan Science and Technology Corporation, Japan

References

1. Prusiner SB. Prions. Proc Natl Acad Sci USA 1998;95: 13363–13383.
2. Berr C, Richard F, Dufouil C, et al. Polymorphism of the prion protein is associated with cognitive impairment in the elderly: the EVA study. Neurology 1998;51:734–737.
3. Dermaut B, Croes EA, Rademakers R, et al. PRNP Val129 homozygosity increases risk for early-onset Alzheimer's disease. Ann Neurol 2003;53:409–412.
4. Combarros O, Sanchez-Guerra M, Llorca J, et al. Polymorphism at codon 129 of the prion protein gene is not associated with sporadic AD. Neurology 2000;55:593–595.
5. Casadei VM, Ferri C, Calabrese E, et al. Prion protein gene polymorphism and Alzheimer's disease: one modulatory trait of cognitive decline? J Neurol Neurosurg Psychiatry 2001;71: 279–280.
6. Shibuya S, Higuchi J, Shin RW, et al. Codon 219 Lys allele of PRNP is not found in sporadic Creutzfeldt-Jakob disease. Ann Neurol 1998;43:826–828.
7. Saunders AM, Strittmatter WJ, Schmechel D, et al. Association of apolipoprotein E allele epsilon 4 with late-onset familial and sporadic Alzheimer's disease. Neurology 1993;43:1467–1472.
8. Johnson GC, Esposito L, Barratt BJ, et al. Haplotype tagging for the identification of common disease genes. Nat Genet 2001;29: 233–237.
9. Suh GH, Shah A. A review of the epidemiological transition in dementia—cross-national comparisons of the indices related to Alzheimer's disease and vascular dementia. Acta Psychiatr Scand 2001;104:4–11.

DOI: 10.1002/ana. 10748

Human Molecular Genetics, 2003, Vol. 12, No. 16 **1945–1958**
DOI: 10.1093/hmg/ddg211

Ubiquitin carboxy-terminal hydrolase L1 binds to and stabilizes monoubiquitin in neuron

Hitoshi Osaka[1,2,†,‡], Yu-Lai Wang[1,†], Koji Takada[3], Shuichi Takizawa[1,4], Rieko Setsuie[1,5], Hang Li[1], Yae Sato[1,5], Kaori Nishikawa[1], Ying-Jie Sun[1], Mikako Sakurai[1,5], Takayuki Harada[1], Yoko Hara[1,6], Ichiro Kimura[6], Shigeru Chiba[4], Kazuhiko Namikawa[7], Hiroshi Kiyama[7], Mami Noda[5], Shunsuke Aoki[1] and Keiji Wada[1,*]

[1]Department of Degenerative Neurological Diseases, National Institute of Neuroscience, National Center of Neurology and Psychiatry, Kodaira, Tokyo, 187-8502, Japan, [2]Information and Cellular function, PRESTO, Japan Science and Technology Corporation (JST), Kawaguchi, Saitama 332-0012, Japan, [3]Department of Biochemistry 1, Jikei University School of Medicine, Minato-ku, Tokyo, 105-8461, Japan, [4]Department of Psychiatry and Neurology, Asahikawa Medical College, Asahikawa, 078-8510, Japan, [5]Laboratory of Pathophysiology, Graduate School of Pharmaceutical Sciences, Kyushu University, Higashi-ku, Fukuoka, 812-8582, Japan, [6]Department of Basic Human Science, School of Human Science, Waseda University, Tokorozawa, 359-1192, Japan and [7]Department of Anatomy and Neurobiology, Graduate School of Medicine, Osaka City University, Abeno-ku, Osaka, 545-8585, Japan

Received March 13, 2003; Revised June 6, 2003; Accepted June 17, 2003

Mammalian neuronal cells abundantly express a deubiquitylating enzyme, ubiquitin carboxy-terminal hydrolase 1 (UCH L1). Mutations in UCH L1 are linked to Parkinson's disease as well as gracile axonal dystrophy (*gad*) in mice. In contrast to the UCH L3 isozyme that is universally expressed in all tissues, UCH L1 is expressed exclusively in neurons and testis/ovary. We found that UCH L1 associates and colocalizes with monoubiquitin and elongates ubiquitin half-life. The *gad* mouse, in which the function of UCH L1 is lost, exhibited a reduced level of monoubiquitin in neurons. In contrast, overexpression of UCH L1 caused an increase in the level of ubiquitin in both cultured cells and mice. These data suggest that UCH L1, with avidity and affinity for ubiquitin, insures ubiquitin stability within neurons. This study is the first to show the function of UCH L1 *in vivo*.

INTRODUCTION

The small 76-amino acid protein ubiquitin (Ub) plays a critical role in many cellular processes, including the cell cycle, cell proliferation, development, apoptosis, signal transduction and membrane protein internalization (1). Moreover, Ub and/or Ub-containing protein aggregates are hallmarks of various neurodegenerative conditions (2). Fundamentally, monoubiquitylation constitutes a sorting signal for membrane proteins to the endosome–lysosomal pathway while polyubiquitylated proteins (covalently linked to Lys48 of Ub) are targeted to the 26S proteasome for degradation. At least three classes of enzymes are engaged in the ubiquitylation processes, namely the E1 (Ub-activating), E2 (Ub-conjugating) and E3 (Ub ligase) enzymes (1). Ubiquitylation also controls the sorting and localization of certain proteins in a reversible manner, much as phosphorylation modulates changes in the structure, activity and the localization of the target proteins. As such, deubiquitylating enzymes (DUBs) act analogously to phosphatases that function in phosphorylation processes (3).

DUBs are subdivided into Ub C-terminal hydrolases (UCHs) and Ub-specific proteases (UBPs). Both classes are thiol proteases that hydrolyze the isopeptide bond between the substrate and the C-terminal Gly76 of Ub. UCHs can hydrolyze bonds between Ub and small adducts or unfolded polypeptides *in vitro* (4). UCHs also can cleave Ub gene products very slowly

*To whom correspondence should be addressed at: Department of Degenerative Neurological Diseases, National Institute of Neuroscience, NCNP, Kodaira, Tokyo, 187-8502, Japan. Tel: +81 423461715; Fax: +81 423461745; Email: wada@ncnp.go.jp
†The authors wish it to be known that, in their opinion, the first two authors should be regarded as joint First Authors.
‡Present address:
Division of Neurology, Clinical Research Institute, Kanagawa Children's Medical Center, Yokohama, 232-8555, Japan.

in vitro, either tandemly conjugated Ub monomers (UbB, UbC) or Ub fused to small ribosomal proteins (L40, S27a), to yield free Ub or ribosomal proteins, respectively (4,5). Yeast expresses one UCH (YUH1) and 16 UBPs (Ubp1–16). Two YUH1 homologs, UCH L1 and UCH L3, have been characterized in mammals (6,7). UCH L1 and UCH L3 are both small proteins of ~220 amino acids that share more than 40% amino acid sequence identity. However, the distribution of these isozymes is quite distinct in that UCH L3 is expressed ubiquitously while UCH L1 is selectively expressed in neuronal cells and the testis/ovary (6,7).

UCH L1 is one of the most abundant proteins in the brain (1–5% of total soluble protein) and immunohistological experiments demonstrate that it is localized exclusively to neurons (6). Although the role of UCH L1 *in vivo* remains unclear, its abundance and specificity for neurons predict a role in neuronal cell function/dysfunction. Similar to Ub, UCH L1 is a constituent of cellular aggregates that are indicative of neurodegenerative disease such as Lewy bodies in Parkinson's disease (PD) (8). Indeed, an isoleucine-to-methionine substitution at amino acid 93 of UCH L1 was reported in a family with a dominant form of PD (9). We found that a *Uch l1* gene deletion in mice causes gracile axonal dystrophy (*gad*), a recessive neurodegenerative disease (10,11). These two examples of neurological disorders in both humans and mice prompted us to investigate the function of UCH L1 in neuronal cells.

We show here that the *gad* mouse is analogous to a *Uch l1* null mutant. Using this mouse and *Uch l1* transgenic mice, we report a novel *in vivo* role for UCH L1 in Ub homeostasis that was unexpected from previous *in vitro* work (12,13). Our data show that UCH L1 associates with Ub in neuronal cells and suggest that this association is important for the maintenance of mono-Ub levels in neurons. UCH L1 effectively upregulates Ub levels at the post-translational level, and this upregulation is probably based on the inhibition of Ub degradation by UCH L1.

RESULTS

UCH L1 is undetectable in the *gad* mouse

The *gad* mouse carries a deletion of a genomic fragment including exons 7 and 8 of *Uchl1* (10). Given such a substantial deletion, the protein encoded by the *gad* allele most likely lacks the core structure of UCH L1, thus predicating its instability [wild-type mouse UCH L1 was modeled using the crystal structure of human UCH L3 (14) as a template; see Fig. 1A]. Immunoblotting using polyclonal antibody to UCH L1 failed to detect UCH L1 in either soluble (10) or insoluble brain lysates from the *gad* mouse (data not shown). Thus, the *gad* mouse is analogous to a *Uch l1* null mutant. Next, we examined whether UCH L3, another UCH in the brain, is upregulated by this mutation. The *gad* mouse showed comparable levels of UCH L3 mRNA and protein (Fig. 1B). Therefore, the phenotype in the mouse does not appear to be modified by compensatory UCH L3 up-regulation. We then employed this mutant mouse to characterize UCH L1 substrates or associated proteins *in vivo*.

UCH L1 associates with Ub

There should be physiological substrates for UCH L1 that accumulate in the *gad* mouse. To facilitate isolation of such UCH L1 substrates or associated proteins, mutant UCH $L1^{C90S}$ was purified from an *E. coli* expression system. UCH $L1^{C90S}$ lacks Ub carboxy-terminal hydrolase activity but retains the ability to associate with Ub (4) (Table 1). As such, UCH $L1^{C90S}$ represented an ideal tool for the purpose of binding to and isolating *in vivo* protein substrates or associates for UCH L1. His-UCH $L1^{C90S}$ and Ni-Sepharose resin were employed in a pull-down assay using soluble brain lysates from wild-type and *gad* mice. Eluates from the resin were subjected to SDS–PAGE and SELDI (surface-enhanced laser desorption/ionization) time-of-flight (TOF) analysis. Relative to wild-type lysates, consistently elevated levels of proteins were not detected in the *gad* mice brains including putative substrates of poly-Ub. Rather, the level of an ~8 kDa protein was consistently lower in *gad* mice lysates (Fig. 1C; left panel; band intensity of *gad* to wild-type is 0.80 ± 0.09, $n = 3$). In both lysates, this protein band was immunoreactive with an antibody to Ub (Fig. 1C; right panel). In-gel digestion of this band followed by tandem liquid chromatography/mass spectrometry produced two peptide sequences—TLSYNIQKESTLHLVLR and TITLEVEPSDTIENVK—that were 100% identical to sequences within mouse Ub. In another pull-down assay, His-Ub pulled down a band corresponding to UCH L1 (Fig. 1D). SELDI analysis showed identical mass peak patterns for the Ub band from wild-type and *gad* mice (Fig. 1E) with a principal mass peak at 8560.8 *m/z*, consistent with the *m/z* expected for free mono-Ub (8564.8). Wild-type and *gad* mouse brain lysates were then subjected to gel filtration chromatography and immunoblotted with anti-UCH L1 or anti-Ub. In the fractions from the wild-type mouse, mono-Ub eluted over the range of ~10–50 kDa, overlapping significantly with the elution of UCH L1 (Fig. 1F). In fractions from the *gad* mouse, however, mono-Ub eluted exclusively at ~10–14 kDa. These data suggest that UCH L1 associates with mono-Ub.

Loss of UCH L1 decreases the level of Ub in neuron

The expression and localization of UCH L1 and mono-Ub in the mouse nerve system were examined. The nervous system is consisted of two types of cells, nerve cells (neurons) and glia (astrocytes, oligodendrocytes/schwann cells, microglia, ependymal cells). Immunofluorescence microscopy shows UCH L1 co-expresses with a neuron marker, neurofilament (NF), but not with an oligodendrocytes marker, proteolipid protein (PLP), and an astrocytes marker, glial fibrillary acidic protein (GFAP), thus supporting the neuron-specific expression of UCH L1 (6) (Fig. 2A). Then double immunofluorescence labeling was performed in neural tissue using UCH L1 antibody and polyclonal Ub antibody that predominantly recognizes free Ub (Sigma) (15). It was found that immunoreactivities to anti-UCH L1 and anti-Ub colocalized within the neuron (Fig. 2B, upper panel). Moreover, Ub immunoreactivity was reduced in neurons in *gad* mice (Fig. 2B, lower panel). In the peripheral nerve, neuronal axons are enwrapped by myelin of glial schwann cells that are immunoreactive to myelin basic protein antibody (Fig. 2C, right and left panels). Immunohistochemisty

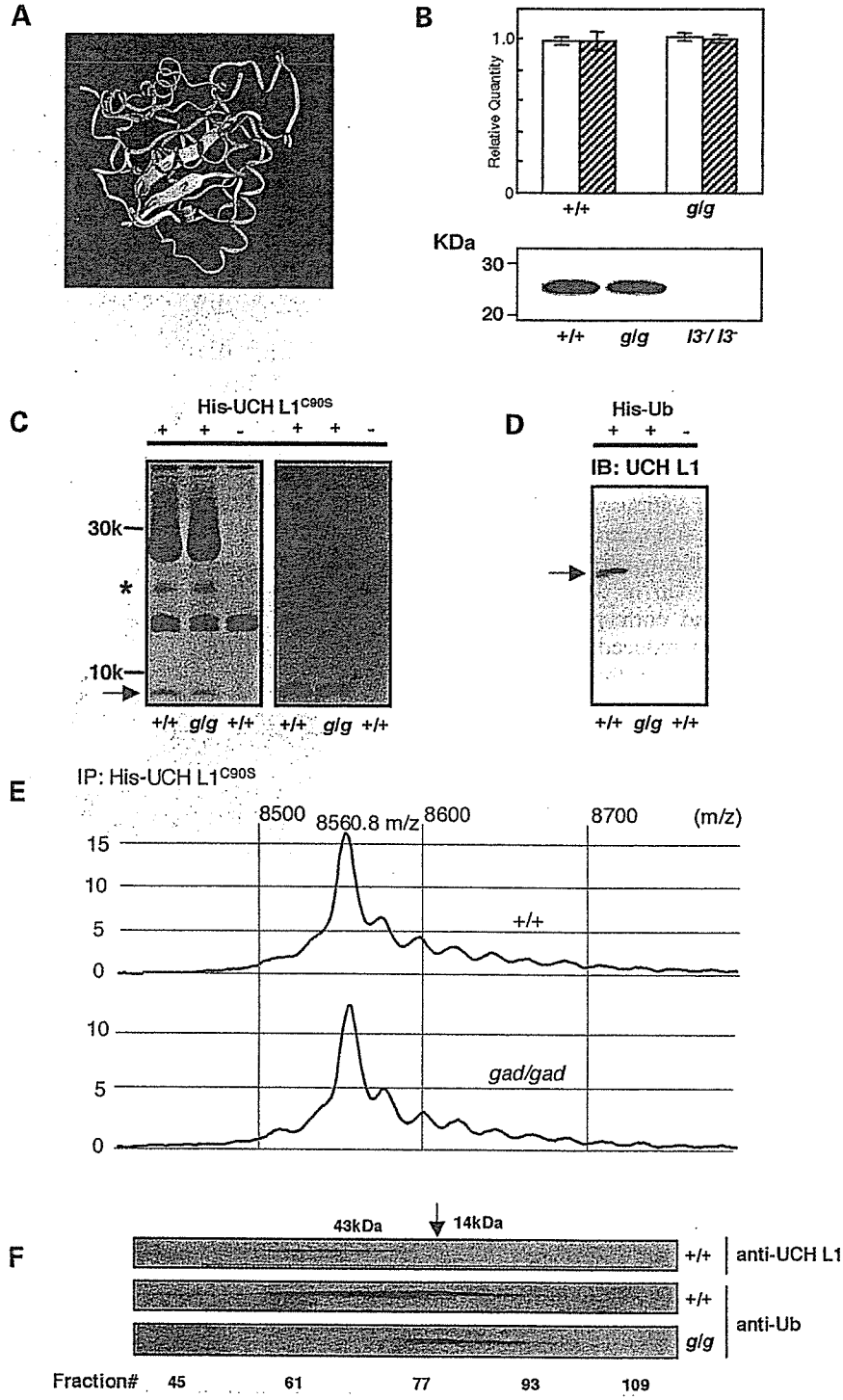

Figure 1. UCH L1 associates with ubiquitin. (**A**) Mouse UCH L1 was modeled after the crystal structure of human UCH L3 (14) using Insight II/Modeler (SGI). Secondary structures of the peptides deleted in the gracile axonal dystrophy (*gad*) mouse are shown in yellow. (**B**, upper panel) Quantitative RT–PCR for *Uch l3* was performed using total RNA from wild-type and *gad* (*gad/gad*) cerebra ($n = 3$ each). Mean values are shown with SEM. β-Actin (open bar) or GAPDH (solid bar) were used as internal controls. (B, lower panel) Soluble fractions (20 μg) of wild-type (+/+), the *gad* (g/g) and *Uch* $l3^{43\text{-}7}$/*Uch* $l3^{43\text{-}7}$/($l3^{-}$/$l3^{-}$) (38) mouse brains were subjected to SDS–PAGE and immunoblotted with anti-UCH L1. (**C**) Eluates from pull-down assays using His-UCH $L1^{C90S}$ and brain lysate were subjected to SDS–PAGE, stained with Coomassie brilliant blue (left panel) and the band intensities to mono-Ub were compared. Eluates were also immunoblotted with monoclonal anti-Ub (right panel; Chemicon). Arrow shows the bands corresponding to mono-Ub. Asterisk shows the non-specific band that is co-purified during UCH L1 purification. (**D**) Eluates from pull-down assays using His-Ub and brain lysate were subjected to SDS–PAGE and immunoblotted with anti-UCH L1. The arrow shows the band corresponding to UCH L1. (**E**) Eluates from pull-down assays using His-UCH $L1^{C90S}$ and brain lysate were desalted with a C_{18} zip tip column and subjected to SELDI analysis. An *m/z* range near that expected for Ub (*m/z* = 8562) is presented. (**F**) Selected gel filtration chromatography fractions from wild-type brain lysates (upper and middle panels) and *gad* mice brain lysates (lower panel) were subjected to SDS–PAGE and immunoblotted with anti-UCH L1 (upper panel) or anti-Ub (middle and lower panels). The arrowhead and arrow correspond to the peak ovalbumin (43 kDa) and ribonuclease A (14 kDa) fractions, respectively.

Table 1. Kinetic parameters for hydrolysis of ubiquitin-7 amid-4 methyl-coumarin (Ub-AMC) by mouse UCH L1 and inhibition by Ub

Enzyme	K_m (μM)	k_{cat} (s^{-1})	$10^6 \times k_{cat}/K_m$ ($M^{-1}s^{-1}$)	K_i (μM)
UCH L1^{WT}	0.16	0.02	0.13	3.3
UCH L1^{D30K}	—	0	0	[0.28][b]
UCH L1^{C90S}	—	0[a]	0	[0.86][b]

Steady-state kinetic parameters were determined at 25°C in assay buffer. The mean values of three independent experiments are shown.
[a]No products were observed after 30 min with 5 mM enzyme.
Inhibitions were not assayed due to the lack of activity to substrates.
[b][Ratio of pulled down Ub to WT].

shows Ub immunoreactivity is decreased in neurons but not at glial schwann cells (Fig. 2D, middle panel).

Subsequently, cytosolic fractions of various nervous tissues that include both neuron and glia were subjected to SDS–PAGE and immunoblotted with a monoclonal Ub antibody that recognizes both free and conjugated Ub in denatured states (Chemicon) (15). The principal band corresponded to free mono-Ub, the intensity of which was reduced in *gad* mouse tissues (Fig. 3A, right panel) suggesting that mono-Ub is decreased in the absence of UCH L1 in the nervous system. A longer exposure or autoclaving the membrane enhanced the bands corresponding to Ub conjugates where no significant differences between wild-type and *gad* mice were observed (data not shown). Then mono-Ub levels in the nervous systems in <2-week-old wild-type and *gad* mice were measured by the radioimmunoassay (13). The inhibition rates for the ^{125}I-mono-Ub bound to antibody US-1 by brain lysates were compared with the standard curve generated by unlabeled mono-Ub (13). US-1 is specific antibody for free mono-Ub (13). Reduced levels of free mono-Ub (~20–30% reduction) were observed in each of the *gad* mouse tissues even at this early age (Fig. 3B; pathology in these mice was apparent only after >6 weeks). Immunoblotting and radioimmunoassay use cell lysates that contain both neuron and glia, which appears to be the reason for the apparent discrepancy between the large difference in Ub immuno-histochemistry in neurons and relatively smaller differences in mono-Ub levels in immunoblotting/radioimmunoassay.

These data show that Ub is associated with UCH L1 in neurons. Absence of UCH L1 reduces the mono-Ub level in neurons, which causes the reduction of overall mono-Ub level in the nervous system.

UCH L1 overexpression increases Ub levels

The effect of UCH L1 overexpression on Ub levels was examined in both cultured cells and transgenic mice. Adenovirus vectors expressing UCH L1 (adeno-*Uch l1*) or β-galactosidase (adeno-β-*gal*) were transfected into mouse embryonic fibroblasts (MEF) cells that do not express UCH L1. After transfection, UCH L1 was induced by Cre recombinase. Reactivitiy to anti-Ub exist at both nucleus and cytosol in adeno β-*gal* transfected and non-transfected MEF cells (Fig. 4B and C). Surprisingly, MEF cells transfected with adeno-*Uch l1* express UCH L1 dominantly at cytosol, where immunoreactivities to anti-Ub and anti-UCH L1

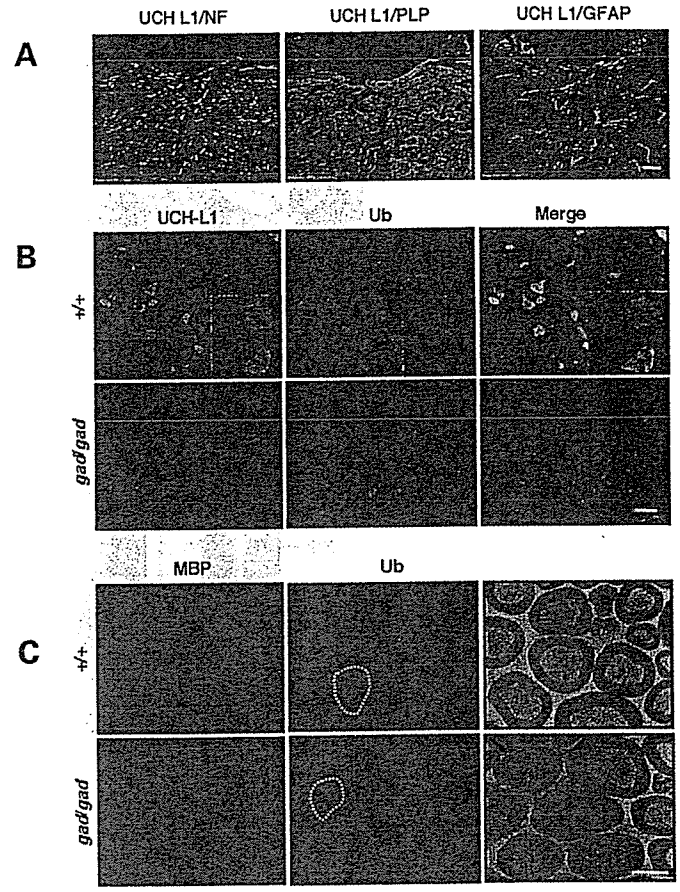

Figure 2. Loss of UCH L1 decreases ubiquitin immunoreactivity. Confocal laser scanning microscopy of mouse brain stem sections (**A**, **B**), sciatic nerve (**C**; left and middle panels) and electron microscopy for sciatic nerve (C; right panels) from 12-week-old wild-type or *gad* mice. (A) Immunohistochemistry to coronal sections at the brain stem, pons (fourth ventricule situates at the upper edges). Antibodies to a neuron marker, neurofilament (NF; left panel, green) and a glial oligodendrocytes marker, proteolipid protein (PLP; middle panel, green) and a glial astrocytes marker, glial fibrillary acidic protein (GFAP; right panel, green) were used for co-immunostaining with anti-UCH L1 (red). Immunoreactivity to anti-NF partially merges with that to anti-UCH L1. NFs exist at neuritis but not at a cell body of a neuron, whereas UCH L1 is expressed at both neuritis and cell bodies. Immunoreactivities to anti-PLP and anti-GFAP do not co-localize with that to anti-UCH L1. Scale bars, 40 μm. (B) Sections at neuronal nucleus in the pons from wild-type (upper panel) and *gad* mice (lower panel) were stained with anti-UCH L1 (green) and polyclonal anti-Ub (red; Sigma) on the same slide. Immunoreactivity to anti-UCH L1 is merged with that to anti-Ub. Moreover, immunoreactivity to anti-Ub is decreased in the *gad* mice that showed no reactivity to anti-UCH L1. Scale bars, 10 μm. Insets are images at four times higher magnification. (C) Sciatic nerve is composed of inner neuronal axon and outer myelin that is immunoreactive to anti-myelin basic protein (MBP, the marker of glial schwann cells, left panels). Immunoreactivity to anti-Ub in the neuronal axon (inside of dashed line) is decreased in the *gad* mouse, whereas the immunoreactivity to anti-Ub in glial myelin (outside the dashed line) is comparable between wild-type and *gad* mice. Electron microscopic images show fine structures of myelin and axon that are similar between wild-type and *gad* mouse in this 12 weeks of age (right panel). Scale bars, 10 μm.

are completely merged (Fig. 4A). Then the levels of Ub were compared by immnoblotting. The level of free mono-Ub as well as ubiquitylated proteins increased relative to the β-*gal* control at 24 h after UCH L1 induction (Fig. 4D; band intensity ratio of

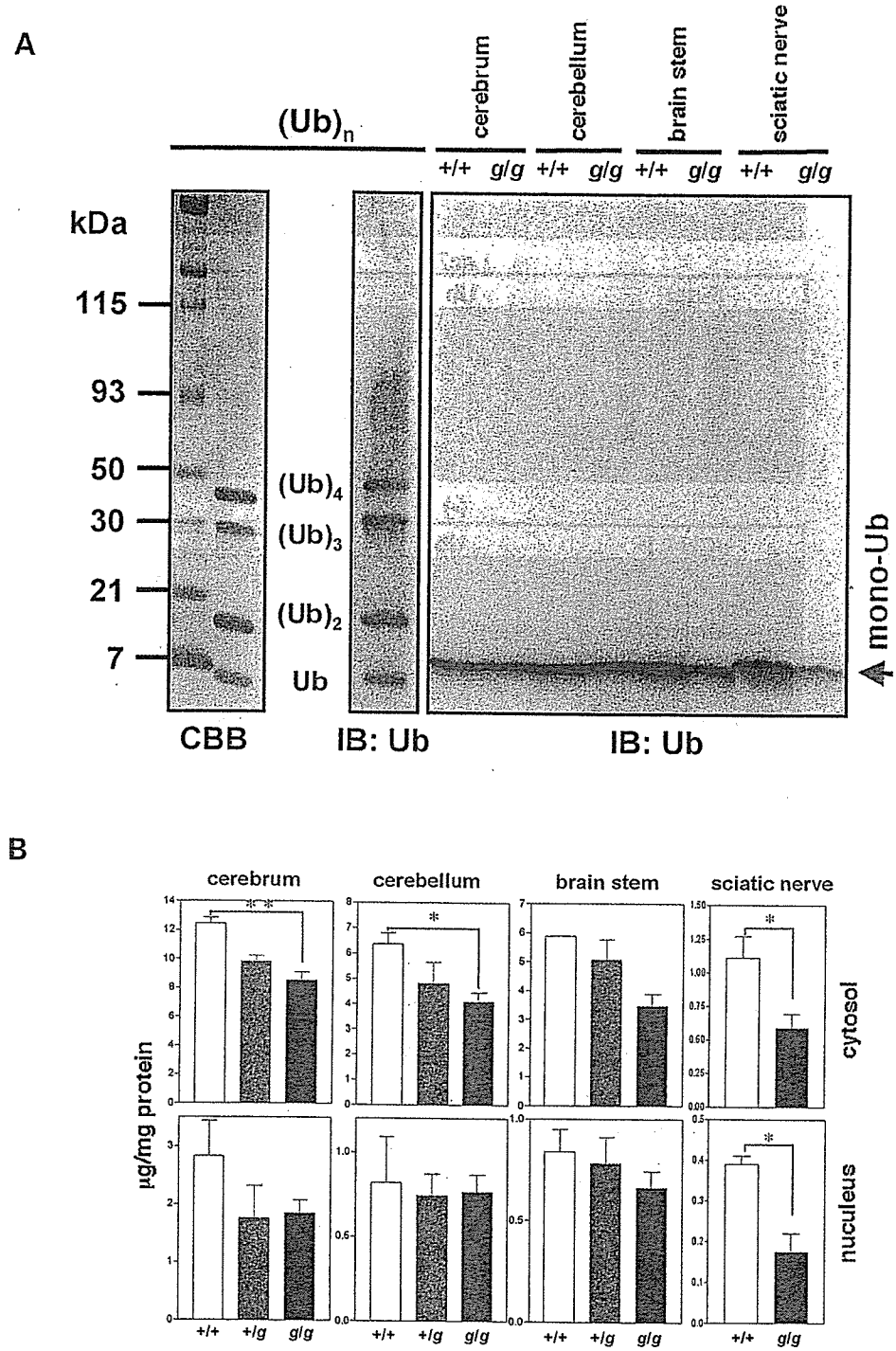

Figure 3. Loss of UCH L1 decreases the level of monoubiquitin. (**A**) A mixture of 1 μg ubiquitin and 4 μg poly-Ub was subjected to SDS–PAGE and stained with coomassie brilliant blue (left panel). Ten percent of this mixture was electrophoresed and immunoblotted with a monoclonal antibody to Ub (Chemicon) that recognizes both conjugated and unconjugated mono-/poly-Ub in denatured states (middle panel). Cytosolic fractions (20 μg) from various neuronal tissues of wild-type and *gad* mice were immunoblotted using the same antibody (right panel). (**B**) Levels of free mono-Ub in cytosolic (upper) and the nuclear (lower) fractions were measured by radioimmunoassay (16) in various brain structures from mice less than 2 weeks old ($n=5$ for cerebrum, cerebellum and brain stem; $n=4$ for sciatic nerve). Mean values with SEM are shown as open (+/+), gray (+/−) or black (*g/g*) bars. $^{**}P<0.01$; $^{*}P<0.05$.

adeno-*Uch l1* transfected cell to β-*gal*-transfected cell were 2.3 ± 0.2 to bands corresponding to mono-Ub and 1.5 ± 0.2 to bands corresponding to MW50-115; $n=3$, corrected by β-actin).

Next, mice carrying a *Uch l1* transgene under control of the EF-1α promoter were generated (Fig. 5A). These mice exhibit no apparent neurological phenotype during life. However, transgenic (Tg) mouse expressing a high copy number of

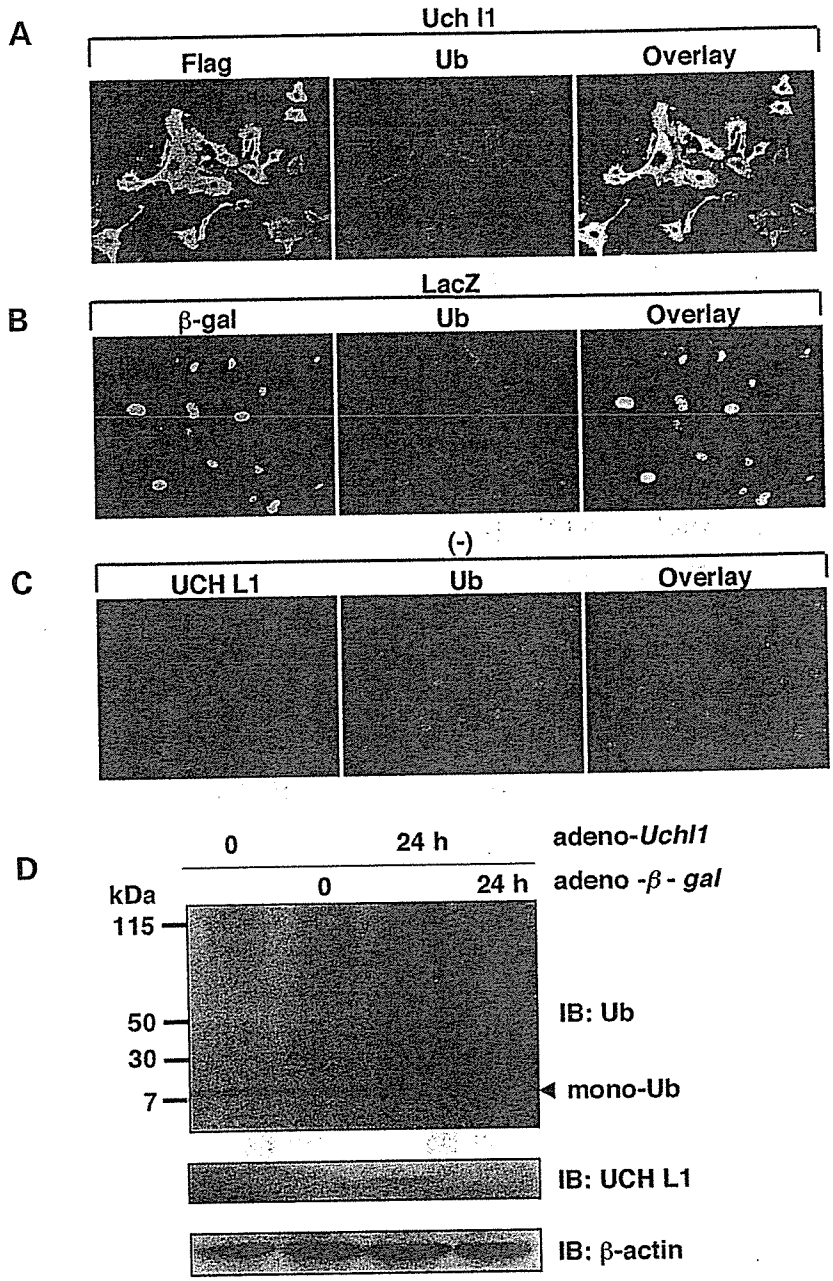

Figure 4. Overexpressed UCH L1 co-localizes with ubiquitin and increases ubiquitin levels in cultured cells. (A–C) E13.5 primary mouse embryonic fibroblasts (MEF) cells were transfected with adenovirus vectors expressing either *Uch l1* (A) or β-gal (B) or not transfected (C). UCH L1 was induced using Cre recombinase for 24 h. Antibodies to flag-tag and β-gal were used for immunostaining to exogenic UCH L1 and β-gal (A, B; left panels). An absence of immunoreactivity to anti-UCH L1 showed the lack of endogenous UCH L1 expression in MEF cells (C; left panel). MEF cells were also labeled with polyclonal anti-Ub (Sigma; A–C; middle panels). Immunoreactivities to anti-Ub/-UCH L1 completely merge in MEF cells transfected with adeno-*Uch l1* (A; right panel), but not in cells transfected with β-gal (B; right panel) and not transfected (C; right panel). Ub localization appears to be recruited to the UCH L1. (**D**) Cell lysates were immunoblotted with anti-Ub (Chemicon) or anti-UCH L1 at the indicated times (upper and middle panels). The same membrane was re-blotted with an antibody to β-actin (lower panel). Band intensities were measured at the bands corresponding to mono-Ub and poly-ubiquitinated bands at MW50-115 kDa and normalized by β-actin intensities.

foreign DNA and high-level of mRNA from *Uch l1* transgene were all infertile ($n = 6$, manuscript in preparation). Therefore, we examined two of these infertile Tg mice, 11 and 22 (Fig. 5B). Immunohistochemistry of brain sections showed increased levels of UCH L1 immunoreactivity in the nervous system of Tg mice (Fig. 5C; left panel, cerebral cortex; right panel, cerebellum). The antibody to Ub that preferentially stains free mono-Ub showed a significant increase in Ub immunoreactivity in Tg mice (Fig. 5D; cerebellum). Immunoblotting also showed the increased level of mono-Ub in Tg mice (Fig. 5E; band intensity for mono-Ub of Tg 22 to wild-type was 2.3 in cerebrum and 1.5 in cerebellum). These data show that UCH L1 overexpression increases the level of mono-Ub in the cultured cells and nervous system *in vivo*.

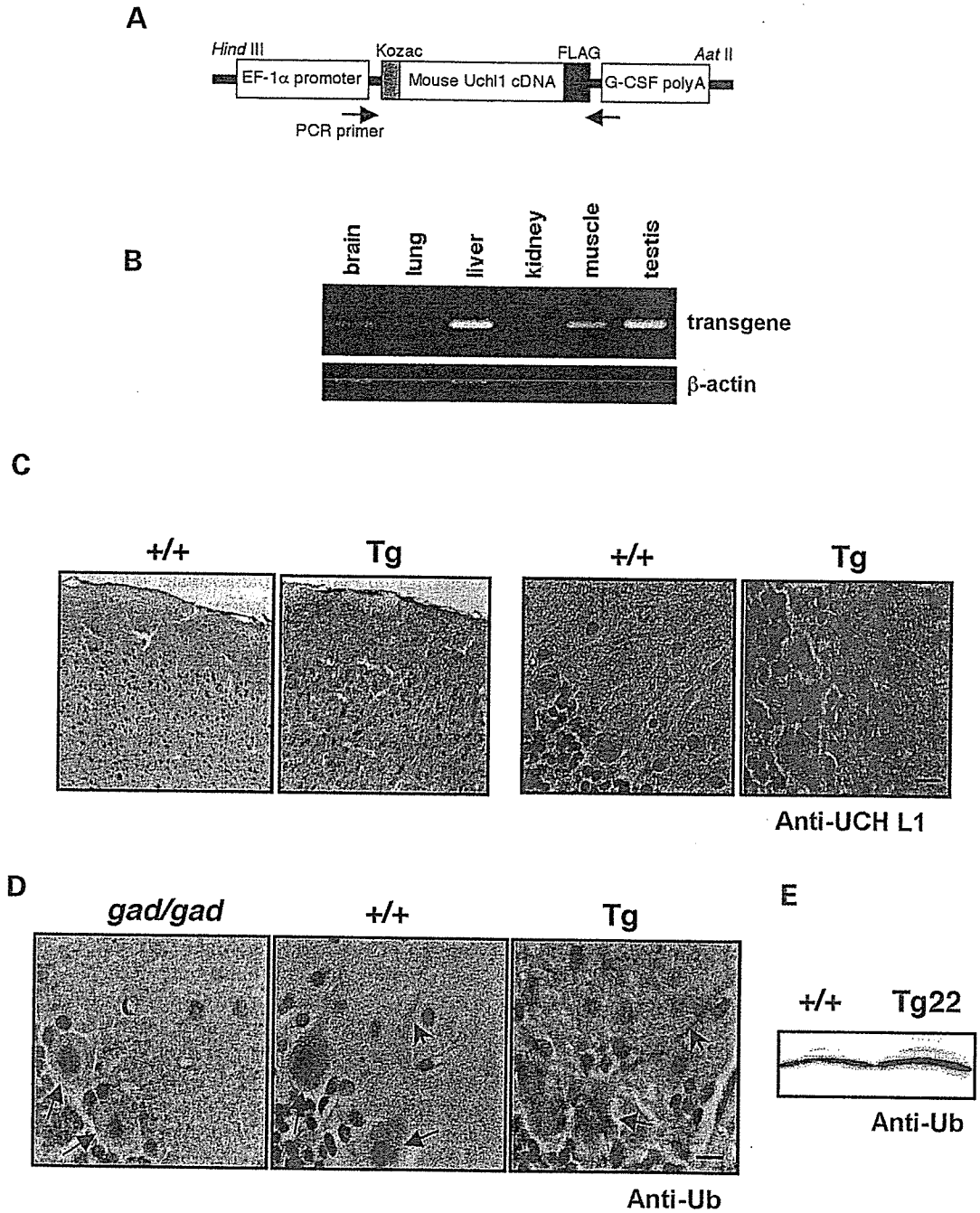

Figure 5. UCH L1 overexpression increases ubiquitin level in the mouse nervous system. (**A**) Construction of the transgenic vector. Flag-tagged mouse *Uch l1* cDNA was subcloned into pEF-Bos vector that carries EF-1α promoter. (**B**) Total RNAs of 5 μg from various organs of transgenic (Tg) mouse 22 were subjected to RT–PCR using specific primers to transgenic *Uch l1* cDNA (upper panel) and β-actin (lower panel). (**C**) Immunohistochemisty to anti-UCH L1 antibody to cerebral cortex (left panels) and cerebellum (right panels) from Tg 22 and wild-type mouse. Scale bars, 20 μm. (**D**) Cerebellar sections from *gad* (*gad/gad*), wild-type (+/+), and UCH L1 transgenic mice (Tg 22) brains were analyzed by immunohistochemistry using polyclonal anti-Ub (Sigma) as the primary antibody. Ub reactivity was increased in Tg 22 mouse. The *gad* mouse showed decreased immunoreactivity to anti-Ub. Arrows and arrowheads indicate Purkinje cell body and neurites, respectively. Scale bars, 20 μm. Twenty micrograms of proteins of the cerebrum (**E**) and cerebellum from Tg 22 and wild-type mouse were subjected to SDS–PAGE and immunoblotted with anti-Ub.

Mechanism by which UCH L1 increases Ub levels

The basis of the UCH L1-mediated increase in Ub levels was examined using three different approaches. First, Ub transcriptional regulation was examined in both wild-type and *gad* mice. The mRNA levels of all four Ub genes, *Uba52*, *s27a*, *UbB* and *UbC*, were analyzed by quantitative PCR but no significant differences were observed between wild-type and *gad* mice (Fig. 6A). A reporter assay using the *UbC* gene promoter also showed no effect of UCH L1 on